Description and phylogenetic relationships of a new specimen of Metriorhynchidae (Crocodylomorpha, Thalattosuchia) from the Kimmeridgian of Switzerland (#80581)

First submission

Guidance from your Editor

Please submit by **12 Jan 2023** for the benefit of the authors (and your token reward) .

Structure and Criteria
Please read the 'Structure and Criteria' page for general guidance.

Custom checks
Make sure you include the custom checks shown below, in your review.

Raw data check
Review the raw data.

Image check
Check that figures and images have not been inappropriately manipulated.

Privacy reminder: If uploading an annotated PDF, remove identifiable information to remain anonymous.

Files
Download and review all files from the materials page.

20 Figure file(s)
3 Table file(s)
5 Other file(s)

Custom checks

New species checks

- Have you checked our new species policies?
- Do you agree that it is a new species?
- Is it correctly described e.g. meets ICZN standard?

Structure and Criteria

Structure your review

The review form is divided into 5 sections. Please consider these when composing your review:

1. **BASIC REPORTING**
2. **EXPERIMENTAL DESIGN**
3. **VALIDITY OF THE FINDINGS**
4. General comments
5. Confidential notes to the editor

You can also annotate this PDF and upload it as part of your review

When ready submit online.

Editorial Criteria

Use these criteria points to structure your review. The full detailed editorial criteria is on your guidance page.

BASIC REPORTING

- Clear, unambiguous, professional English language used throughout.
- Intro & background to show context. Literature well referenced & relevant.
- Structure conforms to PeerJ standards, discipline norm, or improved for clarity.
- Figures are relevant, high quality, well labelled & described.
- Raw data supplied (see PeerJ policy).

EXPERIMENTAL DESIGN

- Original primary research within Scope of the journal.
- Research question well defined, relevant & meaningful. It is stated how the research fills an identified knowledge gap.
- Rigorous investigation performed to a high technical & ethical standard.
- Methods described with sufficient detail & information to replicate.

VALIDITY OF THE FINDINGS

- Impact and novelty not assessed. *Meaningful* replication encouraged where rationale & benefit to literature is clearly stated.
- All underlying data have been provided; they are robust, statistically sound, & controlled.
- Conclusions are well stated, linked to original research question & limited to supporting results.

Standout reviewing tips

The best reviewers use these techniques

Tip	*Example*
Support criticisms with evidence from the text or from other sources	*Smith et al (J of Methodology, 2005, V3, pp 123) have shown that the analysis you use in Lines 241-250 is not the most appropriate for this situation. Please explain why you used this method.*
Give specific suggestions on how to improve the manuscript	*Your introduction needs more detail. I suggest that you improve the description at lines 57- 86 to provide more justification for your study (specifically, you should expand upon the knowledge gap being filled).*
Comment on language and grammar issues	*The English language should be improved to ensure that an international audience can clearly understand your text. Some examples where the language could be improved include lines 23, 77, 121, 128 – the current phrasing makes comprehension difficult. I suggest you have a colleague who is proficient in English and familiar with the subject matter review your manuscript, or contact a professional editing service.*
Organize by importance of the issues, and number your points	*1. Your most important issue* *2. The next most important item* *3. …* *4. The least important points*
Please provide constructive criticism, and avoid personal opinions	*I thank you for providing the raw data, however your supplemental files need more descriptive metadata identifiers to be useful to future readers. Although your results are compelling, the data analysis should be improved in the following ways: AA, BB, CC*
Comment on strengths (as well as weaknesses) of the manuscript	*I commend the authors for their extensive data set, compiled over many years of detailed fieldwork. In addition, the manuscript is clearly written in professional, unambiguous language. If there is a weakness, it is in the statistical analysis (as I have noted above) which should be improved upon before Acceptance.*

Description and phylogenetic relationships of a new specimen of Metriorhynchidae (Crocodylomorpha, Thalattosuchia) from the Kimmeridgian of Switzerland

Léa C Girard [Corresp., 1, 2], **Sophie De sousa oliveira** [2], **Irena Raselli** [1, 3], **Jeremy E Martin** [4], **Jérémy Anquetin** [1, 3]

[1] Department of Geosciences, University of Fribourg, Fribourg, Fribourg, Switzerland

[2] Géosciences Rennes, Université Rennes I, Rennes, Bretagne, France

[3] Jurassica Museum, Porrentruy, Jura, Switzerland

[4] Laboratoire de géologie de Lyon, terre, planète, environnement, UMR CNRS 5276 (CNRS, ENS, université Lyon 1), Ecole Normale Supérieure de Lyon, Lyon, Rhône-Alpes, France

Corresponding Author: Léa C Girard
Email address: lea.girard@unifr.ch

Metriorhynchids are marine crocodylomorphs found all across Jurassic deposits of Europe and Central and South America, mostly as isolated and fragmentary remains. Despite being one of the oldest fossil family named in paleontology, the phylogenetic relationships within Metriorhynchidae are still heavily discussed and have been subject to many revisions over the past fifteen years. Herein, we describe a new metriorhynchid from the Kimmeridgian of Porrentruy, Switzerland. The material consists of a relatively complete, disarticulated skeleton preserving pieces of the cranium, and many remains of the axial and appendicular skeleton. This new specimen is referred to the new species *Torvoneustes jurensis* sp. nov. as part of the large-bodied macrophage tribe Geosaurini. *Torvoneustes jurensis* presents a unique combination of cranial and dental characters including a smooth cranium, a unique frontal shape, acute ziphodont teeth, an enamel ornamentation made of numerous apicobasal ridges shifting to small ridges forming an anastomosed pattern toward the apex of the crown, and an enamel ornamentation touching the carina. The description of this new species allows to take a new look at the currently proposed evolutionary trends within the genus *Torvoneustes* and provides new information on the evolution of this poorly known clade.

Description and phylogenetic relationships of a new specimen of Metriorhynchidae (Crocodylomorpha, Thalattosuchia) from the Kimmeridgian of Switzerland.

Léa C. Girard[1,2], Sophie De sousa oliveira[2], Irena Raselli[3,1], Jeremy E. Martin[4], Jérémy Anquetin[3,1]

[1] Department of Geosciences, University of Fribourg, 1700 Fribourg, Switzerland
[2] Université de Rennes 1, Rennes 35000, France
[3] Jurassica Museum, 2900 Porrentruy, Switzerland
[4] Laboratoire de géologie de Lyon, terre, planète, environnement, UMR CNRS 5276 (CNRS, ENS, université Lyon 1), École normale supérieure de Lyon, 69364 Lyon cedex 07, France

Corresponding Author:
Léa Girard[1,2]
Chemin du Musée 6, 1700 Fribourg, Switzerland
Email address: lea.girard@unifr.ch

Abstract

Metriorhynchids are marine crocodylomorphs found all across Jurassic deposits of Europe and Central and South America, mostly as isolated and fragmentary remains. Despite being one of the oldest fossil family named in paleontology, the phylogenetic relationships within Metriorhynchidae are still heavily discussed and have been subject to many revisions over the past fifteen years. Herein, we describe a new metriorhynchid from the Kimmeridgian of Porrentruy, Switzerland. The material consists of a relatively complete, disarticulated skeleton preserving pieces of the cranium, and many remains of the axial and appendicular skeleton. This new specimen is referred to the new species *Torvoneustes jurensis* sp. nov. as part of the large-bodied macrophagous tribe Geosaurini. *Torvoneustes jurensis* presents a unique combination of cranial and dental characters including a smooth cranium, a unique frontal shape, acute ziphodont teeth, an enamel ornamentation made of numerous apicobasal ridges shifting to small ridges forming an anastomosed pattern toward the apex of the crown, and an enamel ornamentation touching the carina. The description of this new species allows to take a new look at the currently proposed evolutionary trends within the genus *Torvoneustes* and provides new information on the evolution of this poorly known clade.

Introduction

Thalattosuchia Fraas, 1901 is a clade of mostly marine crocodylomorphs that existed from the Early Jurassic to the Early Cretaceous and had a wide distribution from the eastern margins of the Tethys, the opening Atlantic Ocean, and down to the coasts of South America (Fraas, 1901,

1902; Andrews, 1913; Buchy *et al.*, 2006b; Herrera *et al.* 2015; Young *et al.*, 2020a).
Thalattosuchians are subdivided into the more coastal and morphologically conservative Teleosauridae Geoffroy Saint-Hilaire, 1831, and the more pelagic Metriorhynchidae Fitzinger, 1843. Among archosaurs, metriorhynchids show the most advanced morphological adaptations to life at sea, including: limbs transformed into flippers with a great reduction of the forelimbs and a simplification of the pelvic girdle; lengthening of the body; loss of osteoderms; a smooth skin; a hypocercal tail; a slender and lighter skull; hypertrophied salt glands; orbits placed laterally and overhung by the prefrontals; loss of the mandibular fenestra (Fraas, 1902; Gandola *et al.*, 2006; Young *et al.*, 2010; Spindler *et al.*, 2021). This association of characteristics gives metriorhynchids a unique morphology superficially reminding that of ichthyosaurs and dolphins.
Metriorhynchids include two subclades. ~~The~~ Metriorhynchinae Lydekker, 1889 are usually characterized by a slender body, an elongated snout, and a higher count of poorly ornamented teeth (Parrilla-Bel *et al.*, 2013; Sachs *et al.*, 2021). In contrast, ~~the~~ Geosaurinae Lydekker, 1889 are more robust macrophagous predators with shorter snouts and a reduced number of large, strongly ornamented, ziphodont teeth (Young *et al.*, 2012b, 2015). During the Late Jurassic, each of these groups see the emergence of the more derived tribes Rhacheosaurini and Geosaurini, respectively (Young *et al.*, 2013a, b). The diversity of metriorhynchids has long been underestimated, but intensives revisions in the last two decades and the description new material significantly improved the knowledge of the group (Frey *et al.*, 2002; Wilkinson *et al.*, 2008; Young and Andrade, 2009; Andrade *et al.*, 2010; Young *et al.*, 2010, 2020a; Cau and Fanti, 2011). However, the phylogeny of metriorhynchids is still debated (Pierce *et al.*, 2009; Wilberg, 2012; Young *et al.*, 2020b, 2020a).
Compared to its equivalents in England or Germany, the Late Jurassic metriorhynchid fossil record of Switzerland is relatively poor. In addition to the specimen described herein, several specimens of Thalattosuchia have been excavated in the canton of Jura in the past 20 years. They are mainly represented by isolated teeth, but a few well preserved teleosaurid skulls and skeletons are known (Schaefer, 2012; Schaefer *et al.*, 2018). ~~Other, yet~~ unidentified remains of metriorhynchids have been found in the canton of Jura in the form of a nasal, frontal, femur and vertebrae, as well as a single tooth of *Dakosaurus* Quenstedt, 1856 (Schaefer *et al.*, 2018). A metriorhynchid anterior rostrum is also known from the lower Tithonien of Bern representing an indeterminate Rhacheosaurini (Rieppel, 1979, Young *et al.*, 2020b). Here we describe a new specimen from the upper Kimmeridgian of NW Switzerland (Fig. 1). It consists of a relatively complete, associated skeleton with many cranial and postcranial bones preserved. This specimen is identified herein as a new species of the poorly represented genus *Torvoneustes* and replaced in the phylogenetic context of Metriorhynchidae. This material also permits a reassessment of the evolutionary trends previously proposed for the genus.

Materials & Methods

Material

MJSN BSY008-465 consists of a relatively complete, but disarticulated metriorhynchid skeleton (Fig. 2). The specimen was initially collected on a large block of limestone. Bones were prepared directly on the surface and kept on pedestals of rock. This initial phase of preparation, especially the acid preparation, was poorly controlled and resulted in damages of the more fragile bony elements such as some cranial and mandibular elements. More recently, all bones were completely removed from the block to facilitate scientific study. The preserved remains of MJSN BS008-465 include cranial and mandibular elements as well as material from the axial and appendicular skeleton. Many elements are fragmented and show evidence of deformation.
The preserved elements of the cranium include the frontal, prefrontals, right postorbital, nasals, maxillae, right premaxillae. The mandibles are almost complete and preserve both angulars, surangulars, articulars, splenials, and dentaries. Many isolated teeth are also preserved. The postcranial elements include cervical, dorsal, and caudal vertebrae, ribs, the left ischium, the right femur and the right fibula. Numerous bone fragments are not identifiable.

Geological setting

Between 2000 and 2011, controlled paleontological excavations were conducted before the construction of the A16 Transjurane highway in the Canton of Jura (Fig. 1). They revealed the presence of several rich fossiliferous horizons of marls and limestones, as well as several dinosaurs tracksites in the Ajoie region around the city of Porrentruy (Marty *et al.*, 2003). During the Late Jurassic, this region was part of a carbonate platform with diversified shallow depositional environments such as lagoons, reefs, channels and littoral zones forming layers rich in marine fossils (Colombié and Strasser, 2005; Comment *et al.*, 2015).
MJSN BSY008-465 was found in 2008 on the hardground level 4000 of the Lower *Virgula* Marls (Fig. 3) in the locality Courtedoux-Bois de Sylleux, Switzerland (Fig. 1). The Lower *Virgula* Marls belong to the Chevenez Member of the Reuchenette Formation. They are dated from the late Kimmeridgian and correspond to the end of the *Mutabilis* ammonite zone and beginning of the *Eudoxus* ammonite zone (Comment *et al.*, 2015). They are notably characterized by the abundance of the small oyster *Nanogyra virgula*, which gives them their name. The hardground level 4000 is rich in invertebrates, notably encrusted and benthic bivalves and brachiopods. Vertebrates are mostly represented by isolated material, to the exception of the metriorhynchid MJSN BSY008-465 described herein, a partial teleosaurid skeleton provisionally referred to *Steneosaurus* cf. *bouchardi* (Schaefer *et al.*, 2018), and a relatively complete shell of the thalassochelydian turtle *Thalassemys bruntrutana* (Püntener *et al.*, 2015).

Phylogenetic analyses

The phylogenetic analyses were conducted using the data matrix and procedure of Young *et al.* (2020a), which were derived from Young *et al.* (2020b). The original matrix includes 179 taxa coded for 574 characters. The outgroup is *Batrachotomus kupferzellensi*s Gower, 1999. The matrix was modified with Mesquite 3.61 (Maddison & Maddison, 2019) to include MJSN BSY008-465 as a new operational taxonomic unit (see Suplementary data). The latter was scored

for 204 characters. The analytical procedure strictly follows the one described by Young *et al.* (2020a). The parsimony analyses were conducted using TNT 1.5 (No taxon limit) (Goloboff *et al.*, 2008 ; Goloboff & Catalano, 2016) with the RAM increased to 900 Mb. The analysis used the scripts provided by Young *et al.* (2020a) and consisted of an unweighted analysis followed by seven different extended implied weighting analyses (k=1, 3, 7, 10, 15, 20 and 50). The main script (EIW.run) runs an initial "new technology" search (xmult:hits 10 replications 100 rss css xss fuse 5 gfuse 10 ratchet 20 drift 20; sec:drift 10 rounds 10 fuse 3; ratchet:numsubs 40 nogiveup; drift:numsubs 40 nogiveup) holding 20,000 trees per analysis, then runs a "traditional methods" search (bbreak:TBR) on the saved trees. The script then computes the descriptive statistics, the strict consensus tree, the majority rule consensus tree, and the maximum agreement subtree (for more details, see Young *et al.*, 2020a).

The Bayesian analysis was conducted using MrBayes3.2.7 (Ronquist *et al.*, 2012), again following the procedure described by Young *et al.* (2020a). The sampling model is a Markov Chain Monte Carlo with only variable characters scored and a Gama distribution (Mkv+G model). Five independent analyses are run, each with 10 chains for 10 million generations with a sampling every 5000 generations and a burn-in of 40% (for more details, see Young *et al.*, 2020a). ~~At the end of the analysis, the consensus tree is saved.~~

Imaging

Each element of the cranium of MJSN BSY008-465 was individually scanned with a portable surface scanner (Artec Space Spider). The scans were treated with the software Artec Studio 13 to produce textured 3D models. The elements were assembled in Blender 2.8 in order to reconstruct the skull of MJSN-BSY008-465 in 3D (De Sousa Oliveira *et al.*, in press). This technique helped the description and comprehension of the specimen and highlighted lost contacts between the bones. The 3D models of each individual element, as well as the reconstructed skull and mandible are made openly available in De Sousa Oliveira *et al.* (in press).

The microscopic observation and detailed photographs of the teeth of MJSN BSY008-465 were realized with a digital microscope (Keyence VHX-970F).

Institutional abbreviations

BSPG, Staatliche Naturwissenschaftliche Sammlungen Bayerns-Bayerische Staatssammlung für Paläontologie und Geologie, Munich, Germany; IGM, Colección Nacional de Paleontología, Instituto de Geología, Universidad Nacional Autónoma de México; MANCH, Manchester Museum, Manchester, UK; NHMUK, Natural History Museum, London, UK; NHMW, Naturhistorisches Museum Wien, Vienna, Austria; MHNG, Muséum d'histoire naturelle, Genève, Switzerland; MJML, Museum of Jurassic Marine Life, Kimmeridge, Dorset, UK; MJSN, Jurassica Museum (formerly Musée Jurassien des Sciences Naturelles), Porrentruy, Switzerland; NKMB, Naturkunde Museum Bamberg, Bamberg, Germany; MUDE, Museo del

Desierto, Saltillo, Coahuila, Mexico; OUMNH, Oxford University Museum of Natural History, Oxford, UK; SMNS, Staatliches Museum für Naturkunde Stuttgart, Stuttgart, Germany.

The electronic version of this article in Portable Document Format (PDF) will represent a published work according to the International Commission on Zoological Nomenclature (ICZN), and hence the new names contained in the electronic version are effectively published under that Code from the electronic edition alone. This published work and the nomenclatural acts it contains have been registered in ZooBank, the online registration system for the ICZN. The ZooBank LSIDs (Life Science Identifiers) can be resolved and the associated information viewed through any standard web browser by appending the LSID to the prefix http://zoobank.org/. The LSID for this publication is: act:5DEFCF6F-D7EF-4711-9CB6-A7219F612ECB. The online version of this work is archived and available from the following digital repositories: PeerJ, PubMed Central SCIE and CLOCKSS.

Results

Systematic palaeontology

CROCODYLOMORPHA Hay, 1930

THALATTOSUCHIA Fraas, 1901

METRIORHYNCHIDAE Fitzinger, 1843

GEOSAURINAE Lydekker, 1889

GEOSAURINI Lydekker, 1889

Torvoneustes Andrade, Young, Desojo & Brusatte, 2010

Type species: *Dakosaurus carpenteri* Wilkinson *et al.*, 2008

Included valid species: *Torvoneustes coryphaeus* Young *et al.*, 2013b; *Torvoneustes mexicanus* (Wieland, 1910); *Torvoneustes jurensis* sp. nov.

Occurrence : Kimmeridgian of Mexico (Barrientos-Lara *et al.*, 2016); Kimmeridgian of Dorset, UK (Grange and Benton, 1996; Wilkinson *et al.*, 2008, Young *et al.* 2013b); middle Oxfordian to Tithonian of Oxfordshire, UK (Young, 2014); late Kimmeridgian of Canton Jura, Switzerland; upper Valanginian of Moravian-Silesian Region, Czech Republic (Madzia *et al.*, 2021).

Torvoneustes jurensis sp. nov.

urn:lsid:zoobank.org:act:5DEFCF6F-D7EF-4711-9CB6-A7219F612ECB

Figs 2 and 4–16

Diagnosis. *Torvoneustes jurensis* sp. nov. is identified as a member of *Torvoneustes* by the following combination of characters: robust teeth lingually curved, conical crown, bicarinate with a prominent keel; enamel ornamentation made of conspicuous subparallel apico-basal ridges on the basal two thirds of the crown shifting to short, low-relief ridges forming an anastomosed pattern on the apex; carinae formed by a keel and true microscopic denticles forming a continuous row on the distal and mesial carinae; enamel ornamentation extending up

to the carinae near the crown apex; inflexion point on the lateral margin of the prefrontals directed posterolaterally in dorsal view, at an angle of approximately 70° from the anteroposterior axis of the skull; acute angle (close to 60°) between the posteromedial and the lateral processes of the frontal. *Torvoneustes jurensis* differs from the other species of *Torvoneustes* in the following ways: presence of a distinct angle between the anteromedial and the lateral processes of the frontal; smoother overall ornamentation of the skull bones. *Torvoneustes jurensis* also differs from *Torvoneustes carpenteri* in: lacking "finger-like" projections on the posterior margin of the prefrontal; and having a long anteromedial process of the frontal reaching the same level as the anterior margin of the prefrontals (shorter process in *To. carpenteri*). *Torvoneustes jurensis* is also clearly distinct from *Torvoneustes coryphaeus* in having: a tooth enamel ornamentation extending up to the carinae; prefrontals with a rounded distal margin (forming an acute angle in To. coryphaeus); and a supraorbital notch of 90° (45° in To. coryphaeus). The slender morphology, acuteness and great number of teeth of *Torvoneustes jurensis* nov. sp. differs from both *To. coryphaeus* and *To. carpenteri*. *Torvoneustes jurensis* differs from *Torvoneustes mexicanus* in having irregular denticle basal length (120–200µm, mean: 160µm) and distribution (density up to 40 denticles/5mm in the upper middle part of the crown and down to 30 denticles/5mm in the base and apex) on the carinae (regular basal length of 142 µm and density of 30 denticles/5mm in To. mexicanus).

Etymology: The species is named after the Jura, which corresponds to both the mountain range and the Swiss canton from where the holotype was found. The complete name could therefore be translated from Latin as “savage swimmer from Jura”.

Holotype: MJSN BSY008-465, a relatively complete disarticulated skeleton (Fig. 2 and Fig. 4–16).

Type horizon and locality: Courtedoux-Bois de Sylleux, Ajoie, Canton of Jura, Switzerland (Fig. 1). Lower Virgula Marls, Chevenez Member, Reuchenette Formation, late Kimmeridgian (Eudoxus ammonite zone), Late Jurassic (Fig. 3; Comment *et al.*, 2015).

DESCRIPTION

Cranium

Cranial elements are disarticulated except for the frontal preserving its contact with the left prefrontal. The preserved elements of the cranium are exclusively part of the skull roof and snout. Many pieces are fractured, incomplete, and/or deformed. As a result, the general shape and size of most of the skull fenestrae and apertures, such as the preorbital fossae, orbits, and supratemporal fenestrae cannot be clearly determined. Based on the skull reconstruction (Fig. 4), the skull total length is about 88 cm, and the rostrum length (nasals and maxillae) is about 49 cm (55.7% of the total skull length), corresponding to the mesorostrine condition as defined by Young *et al.* (2010). The skull width-to-length ratio is 0.28. The supratemporal fenestrae are greatly enlarged and the orbits are facing laterally (Fig. 4).

Premaxillae.
The right premaxilla is preserved but incomplete. The anterior part is severely damaged. The posterior part is missing so that the contact with the maxilla is not preserved. The external nares aperture is partly preserved, oblong, moderate in width and formed entirely by the premaxilla (Fig. 5d, 5e). A complete lateral alveolus is preserved in ventral view. In dorsal view, the external surface of the bone is smooth except for a few superficial pits. The bone thickens on the external edge of the narial opening and close to the alveolus, but it thins posteriorly. The alveolar orientation suggests a tooth implantation directed anteroventrally (Fig. 4c).

Maxillae.
Both maxillae are preserved. The right maxilla is almost complete, only missing its anteriormost part and the very beginning of the tooth row ~~posteriorly~~ (Fig. 6). This element is heavily fractured and deformed, especially in its anterior part where the bone was broken in several parts and glued back together. The\ three most anterior alveoli are deformed and stretched anteriorly. Remaining matrix prevents the observation of the medial aspect of the right maxilla. The left maxilla is incomplete and broken in four parts. Some of the fragments are severely damaged. The posteromedial process observed on both maxillae is probably formed in part by the palatine. As preserved, the right maxilla is 49.8 cm long. In ventral view, it widens in its posterior region. In lateral and dorsal view, the bone surface is smooth with only pitting ornamentation on its anterior half (Fig. 6). Shallow grooves extend a few millimeters posterior to some of the foramina but are barely visible and can only be spotted on the 3D model. Most other members of the Geosaurini subclade with known maxillae present conspicuous surface bone ornamentation made of grooves and ridges, often with a unique pattern (Young *et al.*, 2013b). *Plesiosuchus manselli* and *To. coryphaeus* both show maxillae ornamented with grooves and raised ridges, while *Dakosaurus maximus* has additional pits to this ornamentation pattern (Young *et al.*, 2012a; Young *et al.*, 2013b). The incomplete maxilla of cf. *Torvoneustes* (MANCH L6459) shows a similar trend to *To. coryphaeus* showing moderate to strong grooves and a raised edge aligned with the sagittal axis of the skull but lack posteroventral foramina (Young, 2014). *Torvoneustes carpenteri* has a pattern of pits and grooves on the lateral edge of its maxilla (Grange and Benton, 1996; Wilkinson *et al.*, 2008). In contrast, MJSN BSY008-465 shows an ornamentation pattern closer to the one seen in *Geosaurus giganteus*, in the form of foramina present as subtle pitting (Young and Andrade, 2009; Young *et al.*, 2013b).
The alveoli are set on a slightly more dorsal plane than the palatal surface of the maxilla ~~immediately medial to them~~. The medial margin of the palatal plate of the right maxilla bears a longitudinal furrow that probably corresponds to the maxillary palatal groove. Each maxilla preserves at least 15 alveoli, which is more than the estimated number of 14 (with 11 strictly preserved alveoli) for *Torvoneustes carpenteri* (Grange and Benton, 1996; Wilkinson *et al.*, 2008; Young *et al.*, 2013b) and less than the estimated alveolar count of 17-19 for *Torvoneustes coryphaeus* (Young *et al.*, 2013b). However, there is at least one or two missing alveoli on MJSN BSY008-465 considering the dentary alveolar count. None of the specimens referred to

the genus *Torvoneustes* preserves a complete maxilla, therefore this character should be treated carefully (see Discussion). Among derived Geosaurini, maxillary alveolar count is usually estimated to be lower than 16 (Table 1; Wilkinson *et al.*, 2008; Young and Andrade, 2009; Young *et al.*, 2012b). The alveoli are large, relatively homogeneous in size, slightly anteriorly oriented and subcircular with a slightly longer anteroposterior axis than their mediolateral axis, which differentiates MJSN BSY008-465 from the members of the informal 'E-clade' taxa (Abel *et al.*, 2020). The interalveolar space is homogeneously narrow, being less than a quarter the length of the adjacent alveoli. Tooth enlargement and interalveolar space reduction are characteristics shared among several members of the Geosaurini subclade (Herrera *et al.*, 2015) like *Dakosaurus, Plesiosuchus* (Young *et al.*, 2012b), some members of the 'E-clade' taxa (Abel *et al.*, 2020) and *Torvoneustes* (Grange and Benton, 1996; Wilkinson *et al.*, 2008; Young *et al.*, 2013b; Young, 2014). The maxillary sutural surfaces with the nasal and premaxilla are visible, presenting gentle slopes of the bone in lateral view. In medial view, the maxilla is concave to accommodate the nasal cavity and thicker around the tooth row. A notch between the 5th and 6th alveoli (Fig. 6a) on the right maxilla could be interpreted as a reception pit but is the only one on the fossil and therefore does not support a tooth-on-tooth vertical interlocking as seen in *Dakosaurus* (Young *et al.*, 2012a) or *Tyrannoneustes lythrodectikos* (Foffa and Young, 2014). In addition, there is no evidence for a maxillary overbite as seen in *Geosaurus giganteus* (Young and Andrade, 2009). It is therefore likely that the tooth occlusion of MJSN BSY008-465 follows the same interdigitated pattern as seen in *To. mexicanus* (Barrientos-Lara *et al.*, 2016).

Nasal

Both nasals are present as symmetrical, unfused elements (Fig 5a, 5b). The right nasal is the best preserved, most complete and less deformed of the two. The nasals are flattened, the left one more so than the right one. The anterior process of the right nasal is curved upward due to postmortem deformation. The posterior part of the right nasal has been fractured then glued back but is not perfectly aligned. This same part is lost in the left nasal. The anterior part of the left nasal is broken and bent laterally. The bone surface is smooth. Only a few elliptical pits are present along the anterolateral parts (Fig. 5a, 5b). This ornamentation pattern differs from the one seen in *To. coryphaeus* (Young *et al.*, 2013b), *P. manselii*, *D. maximus* (Young *et al.*, 2012b), and cf. *Torvoneustes* (MANCH L6459) (Young, 2014). However, it is consistent with other species of Geosaurini with smooth and pitted nasals such as *To. carpenteri* (Grange and Benton, 1996), *Geosaurus grandis, G. giganteus* (Young and Andrade, 2009), and *Dakosaurus andiniensis* (Pol and Gasparini, 2009). The posterolateral part, which should contact the lacrimal, is lost in both nasals. Overall, the nasals are triangular in shape, with the anterior part being elongate and acute. This shape is found in most metriorhynchoids (Andrews, 1913; Lepage *et al.*, 2008). Based on the sutural contacts with the maxillae and the skull reconstruction (Fig. 4), it appears that the nasals do not reach the premaxillae anteriorly. The posteromedial, posterolateral, and anterolateral sutural surfaces of the nasal with the frontal, the prefrontal, and the maxilla, respectively, are well preserved. On the median edge, a subtle angle marks the limit between the

nasal-frontal and the median nasal sutures. The two nasals would contact on the midline of the skull, the medial concavity of the nasals in dorsal aspect suggests the presence of the longitudinal depression at their contact, a metriorhynchoid apomorphy (Young *et al.*, 2012).

Prefrontal

The two prefrontals are preserved, but the anterior parts and the descending process are missing on both. The left prefrontal is still connected with the frontal (Fig. 7) while the right one is found apart (Fig. 5c). The right prefrontal seemingly suffered more damages than the left one, with the bone surface being partially flaked off and the bone flattened and stretched. It has also been broken and glued back together. The left prefrontal shows little deformation but is raised in its anterior part above the level of the frontal, indicating that these bones were crushed and flattened. The posterior part of the descending process on both prefrontals is barely preserved as a thin, concave structure. In dorsal view, the prefrontal is large, laterally extended, and it partially overhangs the orbit (Fig. 4a), a feature common within Metriorhynchidae (Fraas, 1902; Andrews, 1913; Young *et al.*, 2010). The bone surface is smooth with numerous round or elliptical pits, more densely distributed on the anteromedial part (Fig. 5c, 7). As in most metriorhynchids, the posterolateral corner of the prefrontal is rounded in MJSN BSY008-465 (Andrews, 1913; Lepage *et al.*, 2008), which differs from the geosaurines *To. coryphaeus* (Young *et al.*, 2013b) and *D. maximus* (Young *et al.*, 2012a, Pol and Gasparini, 2009) in which the posterolateral corner is angular. The inflection point of this corner is directed posteriorly and forms with the midline of the skull an angle of about 70°, which is found in other Geosaurinae such as *To. carpenteri, D. maximus*, and *D. andiniensis*. A posteriorly directed inflection point of the prefrontal of 70° or less is an apomorphy of the tribe Geosaurini (Cau and Fanti, 2011). If they share a similar shape, the posterior edge of the prefrontals in MJSN BSY0008-465 lacks the "finger-like" projections described in *To. carpenteri* (*Young et al.*, 2013b).

Frontal

The frontal is mostly complete but somewhat flattened (Fig. 7). It consists of a single unpaired element without external sign of a medial suture. Only the anterior most part of the anteromedial process and parts of both intratemporal flanges are missing. The medioventral part of the left lateral process is stretched in the posteromedial direction (Fig. 7). Remaining matrix prevents the observation of the ventral aspect of the frontal. The anteromedial process of the frontal is broad, triangular in shape and extends anteriorly between the nasals. Considering the nasals geometry and preserved sutural contacts (Fig. 4), it is likely that the anterior process of the frontal ended in an acute tip, almost reaching the level of the anterior margin of the prefrontals as seen in cf. *Torvoneustes* (MANCH L6459) and *To. coryphaeus* (Young *et al.*, 2013b; Young, 2014). This differs from the shorter process of *To. carpenteri* (Grange and Benton, 1996; Wilkinson *et al.*, 2008), but the heavy crushing the specimen suffered might induce a bias in the observation of this character. Posteriorly, the frontal presents two lateral processes directed posterolaterally and forming the anterior margin of the supratemporal fenestrae, and a posterior process forming the

anterior part of the intertemporal bar. The opening between the posterior and the lateral processes form an angle of approximately 60°, which is commonly found among ~~the~~ geosaurines whereas metriorhynchines typically show an angle of about 90° (Wilkinson *et al.*, 2008). The posterior process is straight with a constant width of 23 mm. At its posterior end, at the contact with the parietal, two deep grooves form a M-shaped, strongly digitated suture (Fig. 7). The intratemporal flanges (*sensu* Buchy, 2008) extend ventrally from the posterior and lateral processes. They form a triangular area with faint pitting inside the anterior corner of the supratemporal fenestrae. The anterior outline of the supratemporal fossa suggests that it was longer than wide and ovoid in shape, which is a common feature among geosaurines (Buchy, 2008). The supratemporal fenestrae extend far anteriorly and almost reach the level of the interorbital minimal distance. This condition is seen in both *To. carpenteri* and *To. coryphaeus* as well as within *G. grandis* (Foffa and Young, 2014, fig. 9). In dorsal view, the external surface of the frontal is smooth with occasional pitting on the center of the bone, mostly concentrated on the anterior part of the posterior process. This differs from the ornamented frontal of *To. coryphaeus* (Young *et al.*, 2013b), as well as from the anteroposteriorly aligned grooves and ridges observed in the frontal of cf. *Torvoneustes* (MANCH L6459; Young, 2014). In contrast, it resembles the description ~~provided for~~ *To. carpenteri* (Grange and Benton, 1996). In *To. carpenteri* and *To. coryphaeus,* the anterior and lateral processes of the frontal form an almost straight line or a slight concavity (Young *et al.*, 2013b), whereas in MJSN BSY008-465 there is a clear angle of 142° between the processes, measured on the better preserved left side (Fig. 7b). The inflection point is probably located at the meeting point between the frontal, nasal and prefrontal.

Postorbital

Only the part forming the anterolateral margin of the supratemporal fossa of the right postorbital is preserved (Fig. 8a-c). It is broken around its middle and was glued back together. The ventrolateral part, that should make a major part of the postorbital bar, is missing. The posterior part curves slightly laterally but this is probably the result of postmortem deformation. Two processes are distinguishable on what is preserved of the postorbital. The anterior process is anteromedially oriented in dorsal view, making most of the curve of the lateral edge of the supratemporal fossa, and was in contact with the frontal. The posterior process is almost straight, slightly posteromedially oriented, and was in contact with the squamosal. The contact with the lateral process of the frontal is V-shaped, as described in several other metriorhynchids (Andrews, 1913; Foffa and Young, 2014). In the posterior part, the postorbital becomes a thin raised ridge that forms the anterior part of the postorbital-squamosal ridge. Posteriorly, the postorbital-squamosal suture is not readily observable but a change in the bone texture on the medial surface of the bone could match with a similar change on the anterior part of the right squamosal. In medial view, the suture with the frontal is visible, forming a deep incision in the bone (Fig. 8b), which agrees with observations made on complete skulls of other Metriorhynchidae (Andrews, 1913; Young *et al.*, 2013b). This could mark the point where the

postorbital extends medioventrally to take part in the intratemporal flange. Based on the skull reconstruction, the postorbital extends further laterally than the prefrontal, resulting in an enlarged supratemporal fossa as usually seen in metriorhynchids (Wilkinson *et al.*, 2008; Foffa and Young, 2014). The bone surface is unornamented except for one elliptical foramen on the anterior process. ~~There might be another foramen at the corner of the V-shaped suture but it is hard to discern due to poor bone preservation.~~

Squamosal

Both squamosals are present but only represented by their dorsal part. The descending process, which participates to the occipital region, is lost. The right squamosal is the better preserved than the left. In dorsal view, the medial part of the right squamosal is concave (Fig 8f), forming a characteristic L shape (Andrews, 1913; Foffa and Young, 2014; Pol and Gasparini, 2009). The anterior part was in contact with the postorbital. This suture is not readily visible, but a change in bone texture could match with the one seen on the postorbital (see above). A marked ridge separates the squamosal in a medial half that is an area of insertion for the temporal musculature, and a lateral half consisting in a vertical descending surface forming the squamosal flat surface. This ridge forms the posterior part of the postorbital-squamosal ridge, which is present in all Metriorhynchidae but significantly lower among Metriorhynchinae compared to Geosaurinae (Andrews, 1913; Lepage *et al.*, 2008; Pol and Gasparini, 2009; Young *et al.*, 2012b; 2013b; Young and Andrade, 2009). The median process of the squamosal forms the posterolateral corner of the supratemporal fossa and was probably in contact with the lateral process of the parietal (contact not preserved). In its posterior edge, the lateral process is curving slightly upward. The squamosal flat is not as well expressed as the one described for *To. coryphaeus* (Young *et al.*, 2013b) but does resemble the one seen in *D. andiniensis* and *Geosaurus araucaniensis* (Pol and Gasparini, 2009). On both medial and lateral sides there is a foramen in the middle of the bone. In ventral view, the squamosal presents several concavities, identical on both elements that may correspond to portions of the cranioquadrate canal and otic aperture, but they cannot be identified with certainty due to poor preservation.

Parietal

The medial part of the parietal is well preserved, whereas its lateral processes are lost. Like the squamosal, only the dorsal part is preserved. The parts that should connect ventrally with the prootic and the laterosphenoid are not preserved. Upon discovery, the parietal and frontal were still articulated with one another (Fig. 2), but this contact was lost during extraction and preparation. The parietal is a single unpaired element, as usual in crocodylomorphs (Fig. 8d, 8e). Anteriorly, the parietal is of equal width with the posterior process of the frontal then it gradually narrows posteriorly to an extreme degree until it only appears as a raised sagittal ridge, a thalattosuchian condition (Fig. 4, 8e). This narrowing is more pronounced in MJSN BSY008-465 than in *To. coryphaeus* (Young *et al.*, 2013b) and is at least as strong as in *To. carpenteri* (Grange and Benton, 1996), if not more. The anterior process of the parietal forms the posterior

part of the intertemporal bar. Ventrally, the parietal widens to form the posteromedial corner of the supratemporal fossae. As a complete piece, the parietal would be T-shaped in dorsal view with large lateral processes (Andrews, 1913). In lateral view, the anterior process of the parietal slopes down posteriorly, starting from the point where the ridge is the thinnest. From this point, the ridge widens again and forms a triangular area facing posterodorsally. ~~Posteroventrally,~~ the contact with the supraoccipital is not preserved. In palatal view, the posterior part of the parietal is hollow and has one or two foramina on its deepest point.

Mandible

The two mandibular rami are preserved (Fig. 4b). They are relatively complete, but some parts are fractured, eroded, and deformed. Some elements of the mandibles are not articulated anymore. The mandible is represented by several main parts: two ensembles made of the angular, surangular, articular and prearticular; the disarticulated splenials; and the dentaries (preserved in several pieces). The coronoids are lost. The notable absence of a mandibular fenestra is an apomorphy of the Metriorhynchidae (Fraas, 1902; Andrews, 1913; Young *et al.*, 2010). The total length of the mandible is about 815 mm with the anterior end missing. The general shape of the mandible is similar to the one described for *Ty. lythrodectikos* and Geosaurini with the coronoid process located higher than the plan of the tooth row and lower than the retroarticular process, indicating an increase in gape (Young *et al.*, 2012a, 2012b, 2013a).

Dentary

Both dentaries are preserved but not equally well. The left dentary is broken into three parts but is almost complete (Fig. 9), only missing its anteriormost part. The right dentary is broken into two pieces but is highly damaged and deformed. Its ventral and medial parts are completely lost, whereas the posterior part is crushed and deformed. The latter now lies more dorsally and medially compared to the anterior part. The damages are partly due to taphonomic conditions, but also to the poorly controlled acid treatment of the fossil. The left dentary is about 45 cm long, 4.5 cm high and 2.6 cm wide. The right dentary preserves two teeth, including one on its most deformed part with the alveolus deformed and projected inward (Fig. 4b). The left dentary preserves one tooth in the middle of the rostrum (Fig. 9). In dorsal view, the dentary is a long and thick bone. It narrows posteriorly where it was in contact with the angular and surangular. The dentary widens forward starting from the posteriormost alveolus, which is smaller than the one immediately in front. The anterior part of the dentary, including the three anteriormost visible alveoli, curves inward. There are at least 16 clearly identified alveoli, potentially 17, that are overall homogeneous in size. The alveoli are enlarged, subcircular, and slightly longer than wide. The three anteriormost alveoli are larger than the others and lie slightly more dorsally. Overall, the more anterior are the alveoli the more anterodorsally they are oriented. The remaining tooth on the left dentary is anterodorsally directed while the one on the undeformed part of the right dentary is dorsally oriented. The interalveolar space is uniform and greatly reduced, being less than half of the anteroposterior length of the adjacent alveoli. In lateral view, the lateral margin

of the alveoli lies slightly lower than the medial margin except for the three anteriormost alveoli where the lateral and medial margins are on the same plane (Fig. 9b, d). The surangular-dentary groove is visible (Fig, 9b), and does not end anteriorly with a foramen as is the case in *Dakosaurus* (Pol and Gasparini, 2009). A pitting pattern is present on the lateral and ventral surfaces of the dentaries. However, there is no heavy grooving as described in *To. carpenteri* (Wilkinson *et al.*, 2008). At least eight alveoli are adjacent to the symphysis. This count is higher than the four observed in *Dakosaurus maximus* (Young *et al.*, 2012b) but close to Geosaurini indet. (SMNS 80149) from the informal "subclade E" (Abel *et al.*, 2020; Young *et al.*, 2020a) as well as *Plesiosuchus manselli* (Young *et al.*, 2012b). No reception pits for maxillary teeth are observed on the dentaries, indicating that there was no overbite creating a scissor-like occlusion mechanism like in *Geosaurus giganteus* nor any tooth-on-tooth interlocking as seen in *Dakosaurus maximus* (Young *et al.*, 2012a; Young and Andrade, 2009).

Splenial

The left splenial is better preserved than the right one. The two splenials have been flattened and both their anterior and posterior ends are broken. The left splenial is about 37 cm long. In dorsal view, the splenial is narrow on its anterior and posterior ends and thicker in the middle. The lateral edge is straight, but the medial edge is slightly convex (Fig. 10c). The lateral aspect of the splenial is overall concave, with raised ridges forming the sutural contacts with the angular and dentary ventrally, and with the dentary and surangular dorsally (Fig. 10a). The medial surface of the splenial is slightly convex. The ventral edge of the bone is thicker and participates to the ventral edge of the mandible itself. The bone surface is smooth. On the medial surface, a foramen is visible posterior to the thickened part of the bone. The mark of the mandibular symphysis is visible on the anterior third of the splenial, materialized by a rougher surface of the bone (Fig. 10b, 10d). The splenials would contact one another along the symphysis.

Angular and surangular

The angular and surangular are preserved on both sides. They are missing their anterior part and show signs of crushing, erosion and deformation, especially on the left ramus. The angular and surangular are strongly sutured along their entire length. They respectively form the ventral and dorsal halves of the posterior part of the ramus (Fig. 11). In lateral view, the surangular-dentary groove is well expressed. This groove is present in all Metriorhynchidae, albeit not always visible due to deformation, and it is especially deep in the members of the Geosaurini tribe (Pol and Gasparini, 2009; Young *et al.*, 2012b, 2013b; Young and Andrade, 2009). This groove is associated with the passage of the mandibular nerve (Holliday and Witmer, 2007; Young and Andrade, 2009; George and Holliday, 2013) and its posterior end is marked by a foramen. Two other smaller foramina, more or less aligned with the one on the surangular-dentary groove, are found on the posterior part of the surangular, following the upward curve of the bone. The dorsal margin of the surangular rises slightly posteriorly before sloping down after reaching the coronoid process. The coronoid process makes the dorsal part of the anterior half of the

surangular. It stands higher than the tooth row, but lower than the retroarticular process. In lateral view, the coronoid process cannot be differentiated from the surangular. In dorsal view, the coronoid process narrows until its highest point forms a ridge. In medial view, anteriorly the coronoid process forms a low raised ridge on the surangular identified as the surangular medial ridge for the coronoid. The medial surface of the angular and surangular is concave, especially on their anterior part where they would contact the splenial and the coronoid, forming the lateral wall of the Meckelian groove. The large foramen that communicates with the surangular-dentary groove in the lateral surface of the ramus is present below the coronoid process. The angular is thicker than the surangular and forms the ventral margin of the mandible. The posterior part of the angular curves upward toward the retroarticular process forming an angle of approximately 30°. Posteriorly, the angular extends beyond and rises higher than the glenoid fossa to form the ventral part of the retroarticular process.

Prearticular

Only the right prearticular is well preserved. The prearticular is absent in most crocodylomorphs but has been found in many metriorhynchids as well as in a few teleosaurids. Its presence is therefore considered a symplesiomorphy of Thalattosuchia (Andrews, 1913; Martin *et al.*, 2015). The prearticular is a triangular-shaped bone only visible on the medial and dorsal aspect of the ramus (Fig. 11a, 11b). It contacts the angular ventrally, the surangular laterally, and the articular posterodorsally.

Articular

The articular is well preserved only on the right ramus. It contacts the prearticular anteroventrally, the angular posteroventrally, and the surangular laterally. The articular projects far medially. The glenoid fossa, which accommodates the articular condyle of the quadrate, is deep and rounded, and is oriented anterodorsally. The glenoid fossa is divided by a low, rounded rise of the bone oriented anteroposteriorly. It is similar to what have been described in most metriorhynchids and clearly visible in *To. coryphaeus*, which presents a “ridge-and-concavity” morphology to accommodate the “sulcus-and-condyle” of the quadrate (Andrews, 1913; *Young et al.*, 2013b), and opposite to what is seen in *P. manselli* where there is no ridge (Young *et al.*, 2012b). However, in MJSN BSY008-465 instead of a ridge, the separation of the concavities is rather a smooth convexity of the bone. The glenoid fossa is separated from the retroarticular process by a raised ridge similar to the one seen in *To. coryphaeus*. The dorsal surface of the retroarticular process is a smooth posterodorsally oriented concavity which curves medially in dorsal view. It extends laterally beyond the glenoid fossa and slopes downward in medial view. The medial end of the bone is a rugose surface. This description overall matches the one made by Andrews (1913) for Metriorhynchidae. The tip of the retroarticular process is broken, but it would rise higher than the rest of the articular.

Dentition

At least fifteen isolated teeth were found closely associated with the skeleton MJSN BSY008-465. Nine of these isolated teeth are complete, or almost complete, and preserve both the crown and the root. Three additional teeth are still in place on the dentaries and two more on the left maxilla (see above).

Teeth

According to macroscopic observation, teeth correspond to the typical metriorhynchid morphology. They are caniniform, conical, and single-cusped (Massare, 1987; Vignaud, 1997). The teeth are large, robust and bicarenate with the carinae on the anteroposterior axis running continuously from the crown base to the apex. There is no basal constriction of the crown, but the crown-root junction is clearly visible from color and texture (Fig. 12). The tooth roots are at least twice the height of ~~the~~ crown. In cross section, the base of the crown is sub-circular to ovoid with the labial face thicker than the lingual one. The tooth roots are ovoid in cross-section. Closer to the apex, the mediolateral compression of the teeth is increasing. Most tooth crowns are over 20 mm high, but the tooth height is not uniform. ~~The average crown height is 21.94 mm with a standard deviation of 4.38. This calculation includes all of the 15 teeth. It is to be noted that some of them have their apex broken but not enough to significantly affect the crown height.~~ The shortest tooth is 13.23 mm high and the highest is 29.28 mm. ~~The average width at the tooth base is 10 mm (standard deviation 0.9) for a length of 11.36 in average (standard deviation 0.87). The average difference between the width and the length is 1.36 mm (standard deviation 0.93), but the minimal value is 0.3 mm and the maximal value is 3.67 mm with no correlation to the crown height.~~ Teeth are curved lingually and posteriorly. The morphology of the alveoli and the teeth still in place, especially the anterior ones, indicate that teeth were implanted forward in the jaws. Crowns are heavily ornamented with long longitudinal subparallel ridges on at least the basal two thirds of the teeth. Ridges are denser on the lingual face than on the labial one. On the apex, the ornamentation is more discreet and consists of low short ridges forming an anastomosed pattern of drop-shaped ornaments (Figs. 12, 13). This peculiar ornamentation pattern has only been described in other *Torvoneustes* species (Andrade *et al.*, 2010; Young *et al.*, 2013b; Young *et al.*, 2019; Barrientos-Lara *et al.*, 2016) as well as in the teleosaurids *Machimosaurus* Krebs, 1967 and *Lemmysuchus obtusidens* Andrews, 1909 (Johnson *et al.*, 2017). As seen in *Torvoneustes*? (NHMW 2020/0025/0001), the enamel ridges on the upper part of the teeth shift and bend toward the carinae. The carina is well developed, as in other *Torvoneustes* specimens. According to Madzia *et al.* (2021), the developed keel and the shift of enamel ridges toward the carinae are both autapomorphies of *Torvoneustes*. On the basal two thirds of the crown, the carinae are serrated with no involvement of the enamel ornamentation. On the apical third of the crown, there is a clear shift in the enamel ornamentation pattern, and the enamel ridges bend toward the carinae and touch the serrated keel (Fig. 13a). The serration is present from the base of the carinae to the apex and is high, especially on the apical half of the crown. The serration is only faintly visible on macroscopic observation. The tooth apex is sharp, similar to what is described for *Torvoneustes mexicanus* and different from the blunter tooth tips

of *To. carpenteri*, *To. coryphaeus* and *Torvoneustes*? (NHMW 2020/0025/0001) (Barrientos-Lara *et al.*, 2016, Madzia *et al.*, 2021). In an unpublished work on isolated thalattosuchian teeth from the Pal A16 collection, Schaefer (2012) already noted the resemblance of the teeth of MJSN BSY008-465 with the ones of *To. carpenteri*, while pointing out the greater sharpness of the former.

Observed with optic aids, the serration of the carinae is formed by a continuous row of poorly isomorphic, isolated denticles weakly affecting the keel height (poorly developed incipient denticles). This serration corresponds to the microziphodont condition as defined by Andrade *et al.* (2010) with the denticles all smaller than 300 µm in height and length. The denticles base length varies between 120 and 200 µm with an average of 160 µm (Fig. 13), differing from the regular and 142-µm-long (average) denticles of *To. mexicanus* (Barrientos-Lara *et al.*, 2016). The denticle density (amount of denticles/5mm, following Andrade *et al.*, 2010) ranges from 31 to 40 depending on the area on the teeth with an average of 35, which is higher than the average measured on *To. mexicanus* (Barrientos-Lara *et al.*, 2016) and *G. grandis*, but corresponds to the number found on *Geosaurus* indet. (SMNS 81834; Andrade *et al.*, 2010). The denticle density increases in the middle of the tooth crown and decreases at the apex, making the denticles more densely packed and narrower on the part where the carina is the highest. At the apex, the enamel ornamentation joins the carina (Fig. 13a, 13b), similar to the condition in *To. carpenteri* and *To. mexicanus* (Barrientos-Lara *et al.*, 2016; Andrade *et al.*, 2010) and contrary to what is observed in *To. coryphaeus* (Young *et al.*, 2013b; Foffa *et al.*, 2018a). The denticles are harder to discern in this region. This false-ziphodont condition (Prasad and de Lapparent de Broin, 2002) is found in *Torvoneustes* but also in *Machimosaurus* (Andrade *et al.*, 2010; Young *et al.*, 2014). However, the combination of true and false ziphodonty, as defined by Andrade *et al.*, 2010, is only known in *To. carpenteri, To. mexicanus,* and *Torvoneustes* sp. (OUMNH J.50061 and OUMNH J.50079-J.50085) (Young *et al.*, 2013b; Young *et al.*, 2019; Barrientos-Lara *et al.*, 2016). The base of the carina around the upper middle of the tooth shows structures resembling the "inflated base" seen in *To. carpenteri* (Fig. 13b; Andrade *et al.*, 2010). MJSN BSY008-465 does not present the faceted teeth of *Iieldraan* and *Geosaurus* (Young *et al.*, 2013a), nor the macroscopic denticles of *Dakosaurus* (Andrade *et al.*, 2010; Pol and Gasparini, 2009), nor the characteristic flanges on the side of the carinae seen in *Plesiosuchus* (Owen, 1883; Young *et al.*, 2012b).

Tooth count

The holotype of *To. carpenteri* is the only other specimen referred to *Torvoneustes* that has ~~been found with~~ a maxilla as complete as MJSN BSY008-465 (Grange and Benton, 1996). The paratype preserves a dentary, yet just a few fragments and not a complete piece, in contrast to MJSN BSY008-465. On the right maxilla of MJSN BSY008-465, there are at least 15 preserved alveoli (13 on the left one) while there are at least 16 to 17 alveoli on the left dentary and possibly 17 alveoli on the more poorly preserved right dentary. The dentary tooth count is usually lower than the maxillary count. This might indicate at the very least one to two missing alveoli on the right maxilla. Metriorhynchids usually bear three teeth on the premaxilla.

Therefore, this would indicate a dental formula for MJSN BSY008-465 of three premaxillae teeth, 16 to 18 maxillary teeth and 16 to 17 dentary teeth (3+16-18/16-17) for a minimal count, but it is likely that the maxillary tooth count could be even higher. It is therefore closer to the 3+17-19/15-17 estimated for *To. coryphaeus* than the 3+14/14 formula estimated for *To. carpenteri* (Young *et al.*, 2013b). However, it must be noted that no *Torvoneustes* species was found with complete maxillae. Moreover, the skull of *To. carpenteri* is badly crushed, so the estimated tooth count might be underestimated, especially considering that, in *To. coryphaeus*, the maxillary tooth row reaches beyond the anterior margin of the orbit. This is also observed in other geosaurines such as *D. andiniensis, G. giganteus* and potentially *P. manselii* (Young *et al.*, 2013b). Comparison with *To. carpenteri* and MJSN BSY008-465 are limited because the contour of the orbits is completely lost in both.

Tooth wear.

In addition to postmortem fractures, the teeth of MJSN BSY008-465 present signs of macroscopic wear. Several teeth have their apex broken resulting in a flattened and smoothed tip. This type of wear was described in *To. coryphaeus* as an indication of repeated impact against hard surfaces. Some teeth also present signs of enamel spalling wear, mainly represented by triangular facets of broken enamel on the labial face. This type of wear was interpreted as resulting from tooth-food abrasion and was also described in *To. coryphaeus*, *To. carpenteri* and *D. maximus* (Grange and Benton, 1996; Andrade *et al.*, 2010; Young *et al.*, 2012a, 2012b, 2013b).

Postcranial elements

From the postcranial skeleton, many vertebrae and ribs are preserved as well as a few elements of the pelvis and hindlimbs. Despite the number of postcranial elements, no osteoderms were found. The absence of osteoderms is an apomorphy of Metriorhynchidae (Fraas, 1902; Andrews, 1913; Young *et al.*, 2010).

Vertebrae.

MJSN BSY008-465 was found with 22 of its vertebrae including cervicals, dorsals and caudals. The atlas-axis complex is missing as well as the sacral vertebrae. The vertebrae suffered different level of damage and deformation. Some show stretching, with the centrum deflected from its natural, vertical plane and the apophyses not aligned anymore, or crushing with no preferential direction of deformation. This is mainly the case of dorsal vertebrae. All vertebrae are amphicoelous, as in all metriorhynchids (Fraas, 1902). The concavity is shallow and similarly developed in the anterior and posterior articular surfaces.

Cervical vertebrae.

Three post-axis cervical vertebrae are preserved. The number of post-axis cervical vertebrae is considered to be five among Metriorhynchidae, with the fifth cervical closely resembling the first

dorsal (Fraas, 1902). We can therefore assume that the preserved vertebrae are all mid cervicals. Two of them are well preserved, including one complete (Fig 14a, 14b). The centrum is subcircular to ovoid, with the length of the vertebra subequal to the centrum height and width. The neural spine is shorter than the centrum height. As in all thalattosuchians, the cervical vertebrae are amphicoelous. The parapophysis is low on the centrum, ventrally directed, without reaching lower than the ventral margin of the centrum (Fig. 14). A low parapophysis not associated with the neural arch is what characterizes cervical vertebrae (Andrews, 1913; Young *et al.*, 2013a; Parrilla-Bel and Canudo, 2015). The parapophysis ends with a concave articular facet. This facet articulates with the cervical rib. The diapophysis is also low, starting just above the neural arch-centrum suture, and ventrally oriented, reaching below the suture. The neurocentral sutures are not closed. On the ventral margin, on the edges of the articulation surfaces of the centrum, discreet ridges are a sign of muscle attachments. There is a deep concavity between the parapophysis and diapophysis. This strong constriction has also been noted in *Maledictosuchus riclaensis* (Parrilla-Bel and Canudo, 2015). In ventral view, there are two shallow concavities between the parapophyseal processes and the centrum ventral margin, creating a medial keel also described on the cervical vertebrae of *D. maximus* and *Maledictosuchus riclaensis* (Fraas, 1902; Parrilla-Bel & Canudo, 2015). The ventral margin of the centrum is concave in lateral view. The parapophyses project below this margin in the middle of the centrum, but they do not extend more ventrally than the ventral margin of the articular facets. The zygapophyses are well developed, separated, and extended beyond the centrum. The postzygapophyses are wider than the prezygapophyses, but the latter extend further from the centrum. The articular surfaces of the zygapophyses are ovoid and flat. The morphology of the cervical vertebrae is consistent with the ones described for *To. carpenteri*, *Ma. riclaensis* and other metriorhynchids (Fraas, 1902; Andrews, 1913; Wilkinson *et al.*, 2008; Young *et al.*, 2013a; Parrilla-Bel and Canudo, 2015).

Dorsal vertebrae.

At least nine dorsal vertebrae are preserved, none of them with a complete neural spine nor complete diapophyseal processes. All of them are deformed to some extent. In metriorhynchids, the first dorsal vertebra is the one where the parapophysis is no longer on the centrum but on the neural arch (Young *et al.*, 2013a; Parrilla-Bel and Canudo, 2015). The dorsal vertebrae of MJSN BSY008-465 follow the trend observed by Fraas (1902) with a constriction of the middle of the centrum giving it an hourglass shape. The centrum is higher than wide. Its length is subequal to its height. The vertebrae are amphicoelous, with both articular faces overall equally concave, unlike what had been noted in *Tyrannoneustes lythrodectikos* and *To. carpenteri* (Wilkinson *et al.*, 2008; Young *et al.*, 2013a; Parrilla-Bel & Canudo, 2015). On the neural arch, the spine erects vertically in the posterior half of the centrum length. The parapophysis joins the diapophysis on the neural arch to form the anterior extension, like a little step, of the transverse apophysis, as typically observed within Metriorhynchidae (Fig.14c, 14d; Andrews, 1913, fig. 62; Parrilla-Bel & Canudo, 2015). The transverse apophysis extends greatly beyond the centrum on each side. It

is overall straight with a slight ventral concavity. The zygapophyses are well developed, but not as much as the ones on the cervical vertebrae. As in *Tyrannoneustes lythrodectikos*, they project slightly beyond the centrum (Parrilla-Bel and Canudo, 2015). Among the dorsal vertebrae of MJSN BSY008-465, some of them show unfused suture between the centrum and neural arch, indicating a specimen which did not achieved full maturity (a sub-adult; Brochu, 1996). As seen on the cervical vertebra, on the ventral margin of the caudal vertebra the edges of the articulation surfaces of the centrum, discreet ridges are a sign of muscle attachments.

Caudal vertebrae.

In MJSN BSY008-465, only ten caudal vertebrae are preserved. The number of caudal vertebrae can differ greatly between metriorhynchid species but it is usually over 30 (Andrews, 1913; Parrilla-Bel and Canudo, 2015). The size and shape of the preserved vertebrae vary greatly, which suggests that they originate from different parts of the tail (Fig. 14e–h). However, none of them can be associated with the bend of the tail fluke. Three vertebrae with reduced apophysis are associated with the anterior part of the tail (Fig. 14e, f). These caudal vertebrae are hourglass shaped, but the constriction is not as strong as in the cervical and dorsal vertebrae. Their centrum presents a ventral keel, and their length is subequal to their width. The neural spine is overall rectangular in shape and oriented posterodorsally. There is no notch on the anterodorsal portion of the neural spine as seen in *Rhacheosaurus* and *Cricosaurus* Wagner 1858 species *Cricosaurus araucanensis* and *Cricosaurus suevicus* (Fraas, 1902.; Herrera *et al.*, 2013; Parrilla-Bel and Canudo, 2015). The other caudal vertebrae only preserve portions of the neural spine, greatly reduced for some of them, and are interpreted as more posterior in position. The zygapophyses are not preserved. The articular surfaces of the centrum are rounded and slightly concave. On the caudal vertebrae, the suture between the centrum and neural arch is closed.

Ribs

Cervical ribs.

Three cervical ribs are identified. They form short, slender ribs directed posteriorly with an acute end (Fig. 15c–e). The external face forms a ridge starting from the tuberculum and capitulum. The medial face is concave. In lateral view, the ribs are V-shaped.

Dorsal ribs

There are 15 preserved, but fragmentary, dorsal ribs from MJSN BSY008-465. The dorsal ribs are long and slender, ovoid or round in cross section (Fig. 15a, b). The ribs are arched. The medial surface is flat, whereas the lateral surface is rounded. There is a ridge on the posterior surface running down from the tubercular (diapophyseal process). The proximal two thirds are flat on the medial side. In its distal third in lateral view, the rib narrows to form a ridge. On the medial side this part shows a sutural surface. This shift might mark the limit between the vertebrocostal part to the intercostal part of the rib, but no intercostal is sufficiently preserved to

give a better description. Tuberculum and capitulum are not preserved in available ribs. The ribs overall resemble the dorsal ribs of *To. carpenteri* and other metriorhynchids (von Arthaber, 1906; Andrews, 1913; Wilkinson *et al.*, 2008, fig. 7N).

Chevron

At least one chevron is preserved, probably from the posterior part of the tail considering its small size (Fig. 15f, g). In lateral view it is Y-shaped, and in dorsal view it presents two lateral and one medial branches, which corresponds to what has been described in other Metriorhynchidae (Andrews, 1913).

Appendicular skeleton

Ischium

The left ischium is badly preserved, lacking a major portion of its ventral part where the bone would widen the most (Fig. 16c). The proximal part is also missing, as well as the anterior process it should be bearing (Andrews, 1913; Wilkinson *et al.*, 2008). Like in other metriorhynchids, the proximal part is narrow and thick. The neck is measuring 2.5 cm wide. The ischium widens and flattens distally in an overall triangular blade with a thickness of about two millimeters only. The surface of the distal part is covered by striations corresponding to muscular attachment marks on both sides but better expressed on the lateral one.

Femur

The right femur of MJSN BSY008-465 lacks both proximal and distal ends (Fig. 16a, b). It has the sinusoidal shape typically found among Thalattosuchia (Andrews, 1913). The bone is about 24 cm long and 3 cm wide. It is slightly narrower in the middle than at the ends. The medial side is almost flat, whereas the lateral side is convex. The bone flattens toward the distal end. The proximal end, despite the damages it suffered, shows on both sides the rugose surface for muscle attachment commonly found in metriorhynchids (Andrews, 1913; Lepage *et al.*, 2008; Wilkinson *et al.*, 2008).

Fibula

The right fibula is a slender bone about a third of the preserved femur length (Fig. 16d). This ratio is affected by the missing ends of the femur, as well as the missing part of the fibula. The hindlimb proportion in metriorhynchids are often measured with the femur and tibia. According to Andrews (1913), the tibia length being 30% of the femoral length is the general trend found among Oxford Clay metriorhynchids. Within Rhacheosaurini, this ratio is below 30%. The distal end of the fibula is not preserved. The proximal end is damaged but shows a condyle suggesting two tubercles with the posterior one ending higher than the inner one. The inner side is flatter than the outer one, like what is seen in the femur. The bone is one centimeter wide at mid length and enlarged toward both ends, being 2 cm wide at the proximal end.

798
799 **Phylogenetic analysis**
800
801 Following the methodological protocol of Young *et al.* (2020b), the eight parsimony analyses
802 resulted in eight strict consensus topologies with lengths ranking from 2417 steps for the
803 unweighted analysis to 2033 steps for the weakly downweighted topologies (k=20 and k=50; see
804 Table 2). The complete eight strict consensus trees are provided as supplementary material (S1),
805 while descriptive statistics for each of these trees are presented in Table 2. Focusing on the
806 internal relationships of Geosaurinae, four distinct topologies are recovered (Fig. 17). They all
807 have a similar structure, except for the position of *Tyrannoneustes lythrodectikos*, *Ieldraan*
808 *melkshamensis*, *Geosaurus lapparenti*, *Metriorhynchus westermanni*, and *Metriorhynchus*
809 *casamiquelai*.
810 In all of the strict consensus trees, *Torvoneustes jurensis* is included in a polytomous clade with
811 all terminal taxa assigned to *Torvoneustes* (Fig. 17). This clade forms a polytomy with the E-
812 clade and *Purranisaurus potens*. In the unweighted analysis, this group made of *Torvoneutes*, the
813 E-clade and *P. potens* forms a polytomy with *Ty. lythrodectikos* and a clade consisting of
814 Geosaurina + Plesiosuchina (Fig. 17a). These taxa form together the Geosaurini. In the strongly
815 downweighted analyses (k = 1 and k = 3), *M. westermanni* and *M. casamiquelai* assume more
816 basal positions outside of geosaurines (Fig. 17b). *Tyrannoneustes lythrodectikos* is sister group to
817 the E-clade, which corresponds to the 'subclade T' of Foffa *et al.* (2018a). Within Geosaurina, *I.*
818 *melkshamensis* and *G. lapparenti* switch positions. The moderately downweighted analyses (k =
819 7 and k = 10) result in a topology overall consistent with that of the strongly downweighted
820 analyses, except that *M. westermanni* and *M. casamiquelai* regain a basal position among
821 geosaurines (Fig. 17c). In the moderately to weakly downweighted analyses (k = 15, k = 20, and
822 k = 50), *I. melkshamensis* and *G. lapparenti* switch back to the positions they have in the strict
823 consensus of the unweighted analysis (Fig. 17d). Overall, the results of our parsimony analyses
824 are consistent with those of Young *et al.* (2020b) and Abel *et al.* (2020), except our strict
825 consensus for the unweighted analysis that is less well resolved (subclade T only recovered by
826 the weighted analyses).
827 To improve the resolution of relationships, unstable taxa were pruned a posteriori from the
828 consensus trees to produce a maximum agreement subtree for each of the parsimony analysis
829 (see Material and methods). For the unweighted analysis, a total of 13 taxa, including eight
830 geosaurines (*Metriorhynchus brachyrhynchus*, *Tyrannoneustes lythrodectikos*, *Geosaurus*
831 *lapparenti*, *Purranisaurus potens*, Druegendorf merged, English rostrum, *Torvoneustes* sp.,
832 *Torvoneustes mexicanus*), are pruned from the original set of 180 taxa. In contrast, 33 taxa,
833 including 12 geosaurines (*Metriorhynchus brachyrhynchus*, *Neptunidraco ammoniticus*,
834 *Purranisaurus potens*, Druegendorf merged, English rostrum, Mr Passmore's specimen,
835 Chouquet cf hastifer, *Torvoneustes* sp., *Torvoneustes mexicanus*, *Geosaurus grandis*, *Geosaurus*
836 *giganteum*, and *Ieldran melkshamensis* or *Geosaurus lapparenti*), are pruned for the weighted

analyses. The four new topologies obtained for relationships within Geosaurinae are presented in Figure 18.

All maximum agreement subtrees suggest that *Torvoneustes* sp. and *Torvoneustes mexicanus* are unstable taxa. This is probably the result of the partial nature of these terminals represented by single specimens consisting of an incomplete occipital region and a portion of rostrum, respectively. The pruning of these taxa reveals the internal relationships of the *Torvoneustes* clade. *Torvoneustes coryphaeus* is recovered as the most basal taxon in a sister group relationship with a clade consisting of cf *Torvoneustes* and *To. jurensis* + *To. carpenteri* (Fig. 18). From a more general perspective, the internal relationships of the E-clade and Geosaurina are also identified as unstable.

The Bayesian analysis results in a resolved, but poorly supported tree (Fig. 19). *Torvoneustes jurensis* is resolved as the sister taxon of *Torvoneustes carpenteri*. These two species form the most derived clade within the clade *Torvoneustes*. *Torvoneustes mexicanus* is found as the sister taxon of *To. jurensis* + *To. carpenteri*, whereas *To. coryphaeus* appears as the most basal form. Most nodes in the *Torvoneustes* clade and the E-clade are weakly supported. The Bayesian topology for Geosaurini is similar to the one obtained by Young *et al.* (2020b), with only two exceptions: 1) the position of cf. *Torvoneustes* and *Torvoneustes* sp. are switched; 2) *To. mexicanus* and *To. carpenteri* are no longer sister taxa. In our analysis, the node supports within subclade T is slightly lower, which can be explained by the inclusion of *Torvoneustes jurensis* as a new terminal.

The different phylogenetic analyses performed as part of the present study all consistently find *Torvoneustes jurensis* (MJSN BSY008-465) nested within a *Torvoneustes* clade, supporting our identification. Both the Bayesian analysis and the maximum agreement subtrees of the parsimony analyses support a close relationship between *To. jurensis* and *To. carpenteri*.

Discussion

MJSN BSY008-465 assigned to Geosaurinae

The absence of mandibular fenestrae, the orbits facing laterally and overhung by the prefrontals, and the absence of osteoderms (despite the preservation of numerous postcranial remains) unambiguously place MJSN BSY008-465 among Metriorhynchidae (Fraas, 1901, 1902; Andrews, 1913; Young *et al.*, 2010). In this section, we discuss the assignment of this specimen to Geosaurinae.

The dental characteristics of the Late Jurassic metriorhynchids allow to discriminate the Geosaurinae from the Metriorhynchinae. The latter usually have smooth to faintly ornamented teeth with low, non-serrated carinae, whereas geosaurines have smooth to heavily ornamented teeth with high, serrated carinae (Table 1). The presence of prominent serrated carinae appears to be restricted to the Geosaurini tribe. Some geosaurine genera, such as *Dakosaurus* and *Torvoneustes*, can even be identified based on teeth only (Andrade *et al.*, 2010; Young *et al.*, 2013a). MJSN BSY008-465 shares with *Torvoneustes* the presence of conspicuous apicobasal ridges on the first two-thirds of the crown shifting to an anastomosed pattern on the apex, as well

as the bending of the enamel ridges toward the carinae. The teeth of some Rhacheosaurinae (*Cricosaurus* spp., *Maledictosuchus nuyiviianan*) could evoke those of *Torvoneustes* with conspicuous apicobasal ridges on the first two-thirds of the crown, but in their case the apex is smooth and the carinae are low and non-serrated (Sachs *et al.*, 2019; Table 1).

Derived geosaurines, such as *Plesiosuchus*, *Dakosaurus*, *Torvoneustes*, *Geosaurus*, and the E-clade, show an extreme reduction in interalveolar space associated with a reduction of the tooth count and an enlargement of the teeth (Young *et al.*, 2012b, 2013a, 2013b; Abel *et al.*, 2020). Metriorhynchines, including those with a low tooth count such as *'Cricosaurus' saltillensis* (see below), have large and variable interalveolar spaces (Buchy *et al.*, 2013; Young *et al.*, 2020a; Herrera *et al.*, 2021a, 2021b). The only exception is *Gracilineustes leedsi* in which reduced interalveolar spaces are associated with a high tooth count (+30 per maxilla; Young *et al.*, 2013b). MJSN BSY008-465 presents reduced interalveolar spaces associated with moderately enlarged teeth, which corresponds to the condition in derived geosaurines. In addition, the teeth of MJSN BSY008-465 are on average larger than the typical height observed for metriorhynchine teeth, which are usually shorter than two centimeters (Wilkinson *et al.*, 2008; Herrera *et al.*, 2021b).

The tooth count is often used to differentiate geosaurines from metriorhynchines (Young *et al.*, 2013), but it should be noted that the absolute tooth count is known only in a limited number of species (Table 1). Derived geosaurines are usually considered to have 16 or less teeth per maxilla (Cau and Fanti, 2011). With this in mind, the estimated tooth count for MJSN BSY008-465 (17–18 or more, see above) may seem high for a geosaurine, especially when some rhacheosaurines, such as *'Cricosaurus' saltillensis* and *'Cricosaurus' macrospondylus*, present comparable tooth counts (Table 1; Buchy *et al.*, 2013). However, this relatively low tooth count in some racheosaurines seems to be linked to a pronounced shortening of the skull. On the other hand, it appears that the tooth count is poorly estimated in *Torvoneustes* because no complete maxilla is known, and some species have a comparable tooth count as MJSN BSY008-465. For example, *Torvoneustes coryphaeus* is estimated to have up to 19 alveoli per maxilla (Young *et al.*, 2013b), which also falls into the range of other geosaurines such as Chouquet's *Metriorhynchus* cf. *hastifer* and its at least 20 maxillary teeth (Lepage *et al.*, 2008). Therefore, the tooth count for *Torvoneustes* is maybe underestimated for the moment based on the available material. It is also possible that the tendency toward the great reduction in the number of teeth is restricted to the clade uniting Geosaurina, Dakosaurina, and Plesiosuchina. In any case, it appears that tooth count, as a tool for identification, should be handled with care, especially when based on estimations.

MJSN BSY008-465 shares with Geosaurinae the presence of an acute angle of about 60° between the medial and lateral processes of the frontal. This angle is closer to 90° in most Metriorhynchinae, to the exception of *Cricosaurus* in which this angle is around 45°. The new specimen described herein present several additional cranial and mandibular features also found in the macrophagous predators of the Geosaurini tribe: an inflection point of the prefrontals relative to the skull midline of 70° or less; a high glenoid fossa and retroarticular process; a

strongly expressed surangular-dentary groove (Young and Andrade, 2009; Young *et al.*, 2012b; Young *et al.*, 2013b; Foffa and Young, 2014). In addition to some dental characteristics discussed above, MJSN BSY008-465 also presents some cranial features that may recall the metriorhynchine *Cricosaurus*. MJSN BSY008-465 notably has a smooth and unornamented cranial surface, but this is also the case of *Dakosaurus andiniensis*. The frontal of MJSN BSY008-465 differs in shape from that of other geosaurids and somewhat resembles that of *'Cricosaurus' saltillensis* (Buchy *et al.*, 2013), but there is a great diversity of frontal shapes among metriorhynchids (Foffa and Young, 2014, fig. 10; Herrera, 2015). Despite these few similarities, MJSN BSY008-465 lacks some cranial characters that are typical of *Cricosaurus*, such as the presence of a bony septum on the premaxillary and the presence of reception pits on the maxilla (as seen in *C. bambergensis* and *C. albersdoerferi*; Sachs *et al.*, 2019, 2021). Therefore, the craniomandibular characters, like the dental characters, indicate that MJSN BSY008-465 should be assigned to Geosaurinae and suggest that the resemblances with *Cricosaurus* are only superficial.

The total body length of MJSN BSY008-465 is estimated to be around four meters (De Sousa Oliveira *et al.*, in press), which exceeds the sizes typically estimated for *Rhacheosaurus*, *Cricosaurus*, and *Geosaurus*, but falls in the range of *Metriorhynchus* and large-bodied geosaurines such as *Suchodus* and *Torvoneustes*. Since this specimen is one of the few metriorhynchids found with a significant part of its postcranium, some remarks relative to the assignment of the specimen should be made also on this part of the skeleton.

Geosaurinae (*Neptunidraco ammoniticus*, *M. brachyrhynchus*, *Ty. lythrodectikos*, *To. carpenteri*, *Geo. lapparenti*, *D. maximus*) and MJSN BSY008-465 share a centrum length subequal to centrum width on cervical vertebrae, whereas in other Metriorhynchidae (*M. superciliosus*, *Rhacheosaurus gracilis*, *C. araucanensis*, *C. suevicus*, *C. bambergensis*, Solnhofen *Cricosaurus*) the centrum is shorter than wide (see character 423 of the phylogenetic matrix; Parrilla-Bel and Canudo, 2015). In MJSN BSY008-465, the neural spine of the dorsal vertebrae is about half the length of the centrum and its dorsal margin is rounded. This is markedly different from *C. suevicus* and *C. albersdoerferi* in which the neural spine of the dorsal vertebrae is wide and rectangular with a flat dorsal margin and subequal in length to the length of the centrum. The centrum of the dorsal vertebrae is also distinctly longer than high in *C. albersdoerferi*, whereas the centrum length is subequal to its height in MJSN BSY008-465.

In metriorhynchids there is a drastic reduction of the length of the tibia and fibula compared to the femur. The tibia of MJSN BSY008-465 is not preserved, but the fibula is usually subequal or slightly longer than the tibia in metriorhynchids and can therefore be used as a proxy (Sachs *et al.*, 2019). As preserved, knowing that each bone is missing parts of the articular heads, the fibula of MJSN BSY008-465 is about 30% of the femoral length, which corresponds to the proportions usually observed in metriorhynchids. Members of the tribe Rhacheosaurini appear to be an exception because their tibia is less than 30% of the femur length. However, this character (see #518 in the phylogenetic matrix) can only be scored in a small number of metriorhynchids, and its repartition should be further investigated, especially in derived geosaurines such as

Dakosaurus. Although not as diagnostic as the dental and cranial characters, the postcranial characters of MJSN BSY008-465 tend to suggest an affinity of this specimen with geosaurines and to exclude a relationship with rhacheosaurines such as *Cricosaurus*.

Taxonomic diversity in the geosaurine genus *Torvoneustes*.

The genus *Torvoneustes* is a member of geosaurines and is currently represented by three valid species: the type species *To. carpenteri* from the Upper Kimmeridgian, a skull heavily crushed and not described in many details, and some postcranial remains from a second specimen (Grange and Benton, 1996; Wilkinson *et al.*, 2008; Andrade *et al.*, 2010); *To. coryphaeus* from the Lower Kimmeridgian, a nice, 3D preserved skull missing the anterior part of the rostrum (Young *et al.*, 2013b); and *To. mexicanus,* likely from the Kimmeridgian, represented by a piece of a rostrum (Barrientos-Lara *et al.*, 2016). Other specimens were referred to the genus and include three specimens referred to *Torvoneustes sp.* (MJML K1707 from the Upper Kimmerigian, OUMNH J.50061 and OUMNH J.50079-J.50085 from the Lower Tithonian; Young *et al.*, 2019), cf. *Torvoneustes* (MANCH L6459) from the middle Oxfordian (Young, 2014), and *Torvoneustes*? (NHMW 2020/0025/0001) an isolated tooth crown from the upper Valanginian. All specimens are from England, except *To. mexicanus* and *Torvoneustes*?, which are from Mexico and Czech Republic respectively (Table 1).

Based on the three valid species, the genus *Torvoneustes* is defined by the following characteristics (Wilkinson *et al.*, 2008; Andrade *et al.*, 2010; Young *et al.*, 2013b; Barrientos-Lara *et al.*, 2016): great reduction of the interalveolar space; acute angle (around 60°) between the medial and lateral processes of the frontal; inflexion point on the lateral margin of the prefrontals directed posterolaterally at an angle of ~70° from the anteroposterior axis of the skull; circular to subcircular tooth cross section; carina formed by a keel and a contiguous row of poorly defined microscopic denticles difficult to observe even under SEM observation; conspicuous enamel ornamentation consisting of subparallel apicobasal ridges on the first two thirds of the crown shifting to short, low relief tubercles on the apex. The new specimen described herein closely follows this definition, but also presents significant differences with each of the recognized species.

The frontal of MJSN BSY008-465 is shaped differently than those of *To. carpenteri* and *To. coryphaeus*. In *To. carpenteri*, the frontal is shorter than in *To. coryphaeus* and MJSN BSY008-465. *Torvoneustes coryphaeus* has an ornamented frontal while in *To. carpenteri* and MJSN BSY008-465 the frontal is smooth. Finally, MJSN BSY008-465 is characterized by a clear angle between the anterior and posterolateral processes of the frontal, at the meeting point of the frontal, nasals and prefrontals. In the aforementioned two species, there is no visible angle and the processes are aligned in an almost straight line. Variation in shape of the frontals in the genus *Torvoneustes* is not well known, as only two described specimens preserve this element in addition to the new material described herein. Within metriorhynchids, we can note the great interspecific variation in the shape of the frontal (Foffa and Young, 2014). For example in

Cricosaurus, there is a great variation of the frontal shape, as seen in *C. araucanensis* (Herrera, 2015).

MJSN BSY008-465 cannot be compared with *Torvoneustes* sp. (MJML K1707). The latter consists of an incomplete occipital region and this part is completely lost in our specimen. However, MJSN BSY008-465 can be distinguished from all other English specimens. It differs from the type species *To. carpenteri* based on the following characters: smooth maxillae without grooves; anterior process of the frontal reaching the anterior margin of the prefrontals; posterolateral edges of the prefrontals lacking "fringer-like" projections; teeth more slender, curved, and with a sharp apex. MJSN BSY008-465 also differs from *To. coryphaeus* in having: a smooth skull; rounded posterolateral edges of the prefrontals (no acute angle); slender teeth with sharp apex; tooth ornamentation touching the carina in the upper part of the crown. *Torvoneustes* sp. specimens OUMNH J.50061 and OUMNH J.50079-J.50085 preserve incomplete tooth crowns and roots very similar to *To. carpenteri*, As noted above, MJSN BSY008-465 has slender teeth. Finally, MJSN BSY008-465 is different from cf. *Torvoneustes* MANCH L6459 by its smooth cranium.

Torvoneustes mexicanus is only known by a single specimen that consists of a fragment of snout with preserved teeth. The species diagnosis is based only on the teeth with the following characteristics: conical, lingually curved, bicarinate, and more slender than in other *Torvoneustes* species; sharp apex; microziphodont condition with well-defined isomorphic denticles; crown enamel ornamentation consisting of apicobasally aligned ridges on the basal two-thirds of the crown and shifting to short drop-shaped tubercles meeting the carina on the apex (Barrientos-Lara *et al.*, 2016). On macroscopic observation, the teeth of MJSN BSY008-465 and *To. mexicanus* are very similar, but they differ on microscopic ~~observation~~. The denticles of *To. mexicanus* are well defined, regular in shape, size and distribution with a denticle basal length of about 142 µm and a denticle density (#denticles/5mm) of 30 (Barrientos-Lara *et al.*, 2016). The crown height seems to range between 1 and 2.5 cm. In MJSN BSY008-465, the basal length and distribution of denticles are irregular~~. O~~n the tooth total length, the base of the denticles can vary from 120 to 200 µm in length with an average of 160 µm measured on four different teeth~~. Denticles~~ are also more densely packed in the upper middle of the tooth with a density reaching 40 while they can drop to 30 on the basal most part of the carina and the tooth apex. These observations are homogenous on the four observed teeth. It is to be noted however that denticles are sometimes hard to discern, because of their shape and size but also due to areas where they are worn or where the carina is broken. We compared these results with measurements based on formerly published SEM photographs of teeth of *To. carpenteri* (Young *et al.*, 2013a). In this species, the denticle basal length varies between 120 and 220 µm, with most measured denticles having a basal length between 160 and 200 µm. Unfortunately, denticle density cannot be determined. Again based on published SEM photographs (Chiarenza *et al.*, 2015), the denticles of *Torvoneustes*? (NHMW 2020/0025/0002) range in size from 200 to 270 µm in basal length and have a density of 19.

Previous studies showed that the denticle density is variable between geosaurines species such as *Dakosaurus* and *Geosaurus* (Andrade *et al.*, 2010). Measurements took in the middle of the carina gives the following densities for the microziphodont specimens: 28.1 in *Geosaurus* indet. (NHM R.486), and 33.3 for the mesial carina and 41.7 for the distal carina in *Geosaurus grandis*. These results suggest possible interspecific variations in denticles density for a same tooth morphotype among geosaurines and that these variations should not be overlooked for systematic purposes (Andrade *et al.*, 2010). In this study however, the density of denticles is only measured on one tooth. The intraspecific and the individual variation, which were documented in other studies on crocodylomorphs teeth (Prasad and de Lapparent de Broin, 2002), were not explored in this case. However, the observations on MJSN BSY008-465, in addition to previous studies on metriorhynchid teeth, support the idea that microscopic dental characteristics in metriorhynchids have a potential to be used in systematics and should be further investigated. From the above discussion and taking into account that *To. mexicanus* is only known by a very incomplete specimen of uncertain stratigraphical origin, it seems reasonable to conclude that MJSN BSY008-465 represents a different species, which we name here *Torvoneustes jurensis*. Future discoveries of more complete fossil specimens of *To. mexicanus* will allow a better understanding of the differences between these species.

Macroevolution trends in *Torvoneustes*

Young *et al.* (2013b, 2019) discussed macroevolutionary trends in the genus *Torvoneustes*. They first noted a reduction of the maxillary tooth count with time from “relatively high” in cf. *Torvoneustes* (MANCH L6459; Young *et al.*, 2019) and 17–19 in *To. coryphaeus* (Young *et al.*, 2013b), to 14 in *To. carpenteri* (Wilkinson *et al.*, 2008). However, it should be noted that no complete maxilla is known for any specimen referred to *Torvoneustes*, so these tooth counts are ~~just~~ estimations (see above). Another trend noted in *Torvoneustes* is a decrease of dermocranial external ornamentation, with the upper Kimmeridgian *To. carpenteri* having a smoother skull than the older representatives *To. coryphaeus* and cf. *Torvoneustes* MANCH L6459 (Grange and Benton, 1996; Wilkinson *et al.*, 2008; Young *et al.*, 2013b; Young, 2014).

Concerning the tooth morphology, the following macroevolutionary trends were proposed: increasing enamel ornamentation; blunter crown apices; tooth crown losing the lingual curvature; and crown cross section becoming subconical (Young *et al.*, 2019). These trends are interpreted to be linked to an increasingly durophagous diet (Young *et al.*, 2013b; 2019; Foffa *et al.*, 2018b). *Torvoneustes coryphaeus*, *To. carpenteri, Torvoneustes?* (NHMW 2020/0025/0001) and *Torvoneustes* sp. (OUMNH J.50061 and OUMNH J.50079-J.50085) fit relatively well into this proposed evolutionary trend. However, that is not the case of *To. mexicanus* which has more slender teeth than *To. coryphaeus* and *To. carpenteri,* as well as more curved teeth than the latter. The teeth of *To. mexicanus* are also sharper than those of *To. coryphaeus, To. carpenteri* and *Torvoneustes* sp OUMNH J.50061 and OUMNH J.50079-J.50085.

The acquisition of false serration (false ziphodont dentition; Prasad and de Lapparent de Broin, 2002; Young and Andrade, 2009; Andrade *et al.*, 2010) is another macroevolutionary trend

proposed for *Torvoneustes* (Young *et al.*, 2019). *Torvoneustes coryphaeus* is the only species lacking the false ziphodont dentition and is also the eldest specimen whose teeth are known. The other specimens preserving teeth (*To. carpenteri*; *Torvoneustes* sp., OUMNH J.50061 and OUMNH J.50079-J.50085; *Torvoneustes*?, NHMW 2020/0025/0001; *To. mexicanus*) all present the false ziphodont condition. Therefore, the authors propose the acquisition of the false ziphodont condition in all species younger than *To. coryphaeus* (Young *et al.*, 2019).

The discovery of the occipital region of a *Torvoneustes* specimen of great size from the Tithonian of England led Young *et al.* (2019) to propose an increase of body size as a possible evolutionary trend within *Torvoneustes*. This specimen is estimated to be around 6 meters long while other *Torvoneustes* specimens are estimated to be between 3.70 and 4.70 meters long (Young *et al.*, 2011, 2019). And finally, Young *et al.* (2019) also suggested that the increase in length of the suborbital fenestrae leading to an enlarged pterygoid musculature and the ventralization of basioccipital tuberosities would be another evolutionary trend of *Torvoneustes*. However, because this part of the cranium is not preserved in our new specimen, this trend will not be further discussed below.

Torvoneustes jurensis fits relatively well with some of the aforementioned macroevolutionary trends. First, *To. jurensis* is younger than *To. coryphaeus* and indeed presents the false ziphodont condition on its teeth. However, it should be noted that in the current state of knowledge the repartition of this character does not per se corresponds to an evolutionary trend. The false ziphodont condition may be a synapomorphy uniting all *Torvoneutes* species younger than *To. coryphaeus*, or it may be lost in the latter. ~~This should be further explored in a larger phylogenetic context.~~

Torvoneustes jurensis, which is dated from the early late Kimmeridgian, has an even smoother cranium than *To. carpenteri*. Dermocranial ornamentation appears early during ontogeny in crocodylomophs, usually developing in specimens with a skull longer than 200 mm (de Buffrenil, 1982; de Buffrénil *et al.*, 2015). This indicates that the smooth cranium of *Torvoneustes jurensi* is not linked to its ontogenic stage and fits into the evolutionary trend proposed by Young *et al.* (2019). Within Thalattosuchia, the trend toward smoother dermocranial bones is believed to improve hydrodynamic efficiency (Young *et al.*, 2013b) and overall follows the idea that pelagic species have less ornamented skulls than semi-aquatic one (comparing metriorhynchids to teleosaurids for example; Clarac *et al.*, 2017). This trend is also present in *Dakosaurus* with *D. andiniensis*, the geologically younger species, showing smoother cranial bones than *D. maximus* (Pol and Gasparini, 2009; Young *et al.*, 2012a). However, the functional role of bone ornamentation remains controversial in crocodylomorphs (de Buffrénil *et al.*, 2015). Clarac *et al.* (2017) presented evidence that the evolution of ornamentation in pseudosuchians is influenced by both natural selection and Brownian motion. The study shows that heavy ornamentation is present in pseudosuchians with semi-pelagic lifestyle and linked to basking for animals with low mobility. Therefore, the loss of ornamentation in Thalattosuchia may rather be linked to an increasingly pelagic lifestyle than directly to hydrodynamic efficiency.

The description of *To. jurensis* contradicts some aspects of the other proposed evolutionary trends. *Torvoneustes jurensis* presents slenderer and shaper teeth than the other *Torvoneustes* species, except *To. mexicanus*. In their description, Barrientos-Lara *et al.* (2016) raised the question of whether the slender and sharp teeth of *To. mexicanus* could be linked to ontogeny, but the lack of data to characterize ontogenic changes within *Torvoneustes* teeth led them to consider the differences between *To. mexicanus* and other *Torvoneustes* as specific characters. The teeth of *To. jurensis* are very similar to those of *To. mexicanus*. However, the skull length of the holotype of *To. jurensis* is similar to that of the holotype of *To. carpenteri*. Their body length is estimated to be close to 4.0 m for *To. jurensis* and between 4.0 and 4.70 m for *To. carpenteri* (Grange and Benton, 1996; Wilkinson *et al.*, 2008; Young *et al.*, 2011; De Sousa Oliveira *et al.*, in press). Therefore, ontogeny cannot explain the differences in tooth morphology between these species. The sharp and slender teeth of *To. jurensis* and *To. mexicanus* may instead represent a diverging tooth morphotype within the genus. It might indicate that *To. mexicanus* and *To. jurensis* are less specialized than species with more robust teeth. They might be opportunist feeders with durophagous tendencies. *Torvoneustes jurensis* was found in a carbonate platform environment where remains of teleosaurids (*Steneosaurus* and *Machimosaurus*) are abundant, as well as many coastal marine turtles (Thalassochelydia) and hard scale fishes (e.g., *Scheenstia* sp., Figure 20).

The maxillary tooth count of *To. jurensis* is estimated to be at least 16 or 17, but probably higher. Therefore, it seems like the reduction of maxillary tooth count is not a homogenous trend in the genus. However, it should be stressed once more that no definitive maxillary tooth count is known at the moment for any specimen referred to *Torvoneustes*. It is then possibly too early to conclude on any trend for this character.

Regarding the increase in body size, it should be noted that crocodilians continue to grow well into adulthood (Sebens, 1987; Grigg and Kirshner, 2015) and that only a handful of specimens are known for *Torvoneustes*. In these circumstances, any conclusion on size evolutionary trends must therefore be taken with care. As noted above, the holotype specimens of *To. carpenteri* and *To. jurensis* are roughly of comparable total length, which could agree with the proposed evolutionary trend as the two species are roughly of the same age. However, many isolated teeth showing similar characteristics as those of MJSN BSY008-465 were found in the same stratigraphical layers during the excavation on the A16 highway, along with teeth of *Steneosaurus, Machimosaurus* and *Dakosaurus* (Schaefer, 2012; Schaefer *et al.*, 2018) : teeth with sub-circular to ovoid cross-section, bicarinate with micro-ziphodont condition, enamel ornamentation composed of sub parallel apicobasal ridges on the basal two thirds of the crown shifting into low relief drop-shaped ridges forming an “anastomosed pattern” on the remaining upper third of the crown. These teeth show a great variation of height and base length (Schaefer, 2012; pers. obs.). One of these teeth in particular (MJSN TCH007-91) shows a base length 31% longer than the largest tooth associated with MJSN BSY008-465. In addition, the great variation in crown size of isolated teeth indicates that specimens of various sizes (and potentially ages) visited the area, including specimens significantly larger than MJSN BSY008-465. Considering

there is only a few *Torvoneustes* specimens known between the middle Oxfordian and the Tithonian, it seems far-fetched to consider size increase as an evolutionary trend in *Torvoneustes* for the moment.

Conclusions

The holotype of *Torvoneustes jurensis* is the most complete skeleton of the genus and the first to preserve both extensive cranial and post cranial material. This new species is ~~clearly~~ distinct from the other species on the basis of cranial morphology, dental characters, and geographic ~~and temporal~~ repartition. The phylogenetic analysis tends to confirm these observations. The distinction between *To. jurensis* and *To. mexicanus* remains difficult due to the fragmentary nature of the mexican specimen. While future discovery of more specimens of *To. mexicanus* might help to get a better understanding of the differences between these two taxa, the dental characters allow us to discriminate them as two distinct species. It is interesting to note that the genera *Cricosaurus* and *Dakosaurus* are as well found in the Kimmeridgian deposits of Europe, Mexico and South America, but that they are represented by ~~clearly~~ different species in each of these geographically distant areas (Buchy *et al.*, 2006b, 2013; Pol and Gasparini, 2009; Young *et al.*, 2012b; Herrera, 2015; Herrera *et al.*, 2021a). In addition, it seems that the Late Jurassic marine reptiles of the Mexican Gulf are represented by species that differ from the coeval European and South American fauna, with the notable exception of one specimen of *Ophtalmosaurus* (Buchy, 2007; Buchy *et al.*, 2006a). The distinction of *Torvoneustes mexicanus* and *Torvoneustes jurensis* may therefore be seen as another indication that the Mexican Gulf was an isolated environment during the Late Jurassic.

Acknowledgements

The authors would like to thank the Paleontology A16 team for the discovery and initial surface preparation of the specimen, Renaud Roch for his skillful complete extraction of the bones from the matrix, and Davit Vasilyan for the acquisition of the images from the digital microscope. We would also like to thank Corentin Jouault for his help with setting up Bayesian analysis and Mark Young for giving access to the character matrix and TNT script. We also thank the Willi Hennig Society for making TNT freely available.

References

1193 Abel, P., Sachs, S., Young, M.T., 2020. Metriorhynchid crocodylomorphs from the lower
1194 Kimmeridgian of Southern Germany: evidence for a new large-bodied geosaurin lineage in
1195 Europe. Alcheringa: An Australasian Journal of Palaeontology 44(2), p. 312- 326.
1196 Andrade, M.B., Young, M.T., Desojo, J.B., Brusatte, S.L., 2010. The evolution of extreme
1197 hypercarnivory in Metriorhynchidae (Mesoeucrocodylia: Thalattosuchia) based on evidence
1198 from microscopic denticle morphology. Journal of Vertebrate Paleontology 30(5), p. 1451-1465.
1199 Andrews, C.W., 1909. On some new steneosaurs from the Oxford Clay of Peterborough. Annals
1200 and Magazine of Natural History 3, p. 299-308.
1201 Andrews, C.W., 1913. A descriptive catalogue of marines reptiles of the oxford clay. Based on
1202 the Leeds collection in The British Museum (Natural History), London. Part II.
1203 Barrientos-Lara, J.I., Herrera, Y., Fernández, M.S., Alvarado-Ortega, J., 2016. Occurrence of
1204 Torvoneustes (Crocodylomorpha, Metriorhynchidae) in marine Jurassic deposits of Oaxaca,
1205 Mexico. Revista Brasileira de Paleontologia 19(3), p. 415-424.
1206 Brochu, C.A., 1996. Closure of neurocentral sutures during crocodilian ontogeny: Implications
1207 for maturity assessment in fossil archosaurs. Journal of Vertebrate Paleontology 16, 49–62.
1208 Buchy, M.-C., 2008. New occurrence of the genus Dakosaurus (Reptilia, Thalattosuchia) in the
1209 Upper Jurassic of north-eastern Mexico, with comments upon skull architecture of Dakosaurus
1210 and Geosaurus. Neues Jahrbuch für Geologie und Paläontologie - Abhandlungen 249(1), p.1-8.
1211 Buchy, M.-C., 2007. Mesozoic marine reptiles from northeast Mexico: description, systematics,
1212 assemblages and palaeobiogeography. Unpublished PhD thesis, University of Karlsruhe, 98 pp.
1213 Buchy, M.-C., Frey, E., Stinnesbeck, W., López, J.G., 2006a. An annotated catalogue of the
1214 Upper Jurassic (Kimmeridgian and Tithonian) marine reptiles in the collections of the
1215 Universidad Autónoma de Nuevo León, Facultad de Ciencias de la Tiersra, Linares, Mexico.
1216 ORYCTOS 6, 19p.
1217 Buchy, M.-C., Vignaud, P., Frey, E., Stinnesbeck, W., González, A.H.G., 2006b. A new
1218 thalattosuchian crocodyliform from the Tithonian (Upper Jurassic) of northeastern Mexico.
1219 Comptes Rendus Palevol 5, p. 785–794.
1220 Buchy, M.-C., Young, M.T., Andrade, M.B., 2013. A new specimen of Cricosaurus saltillensis
1221 (Crocodylomorpha: Metriorhynchidae) from the Upper Jurassic of Mexico: evidence for
1222 craniofacial convergence within Metriorhynchidae. ORYCTOS 10, p. 9-21
1223 Cau, A., Fanti, F., 2011. The oldest known metriorhynchid crocodylian from the Middle Jurassic
1224 of North-eastern Italy: Neptunidraco ammoniticus gen. et sp. nov. Gondwana Research 19, p.
1225 550–565.
1226 Chiarenza, A.A., Foffa, D., Young, M.T., Insacco, G., Cau, A., Carnevale, G., Catanzariti, R.,
1227 2015. The youngest record of metriorhynchid crocodylomorphs, with implications for the
1228 extinction of Thalattosuchia. Cretaceous Research 9.
1229 Clarac, F., De Buffrénil, V., Brochu, C., Cubo, J., 2017. The evolution of bone ornamentation in
1230 Pseudosuchia: morphological constraints versus ecological adaptation. Biological Journal of the
1231 Linnean Society 121, 395–408. https://doi.org/10.1093/biolinnean/blw034

1232 Colombié, C., Strasser, A., 2005. Facies, cycles, and controls on the evolution of a keep-up
1233 carbonate platform (Kimmeridgian, Swiss Jura): Evolution of a keep-up carbonate platform.
1234 Sedimentology 52, 1207–1227. https://doi.org/10.1111/j.1365-3091.2005.00736.x
1235 Comment, G., Lefort, A., Koppka, J., Hantzpergue, P., 2015. Le Kimméridgien D'Ajoie (Jura,
1236 Suisse) : Lithostratigraphie Et Biostratigraphie De La Formation De Reuchenette.
1237 https://doi.org/10.5281/ZENODO.34341
1238 de Buffrenil, V., 1982. Morphogenesis of bone ornamentation in extant and extinct crocodilians.
1239 Zoomorphology 99, 155–166.
1240 de Buffrénil, V., Clarac, F., Fau, M., Martin, S., Martin, B., Pellé, E., Laurin, M., 2015.
1241 Differentiation and growth of bone ornamentation in vertebrates: A comparative histological
1242 study among the Crocodylomorpha: Development of Bone Ornamentation In The
1243 Crocodylomorpha. J. Morphol. 276, 425–445. https://doi.org/10.1002/jmor.20351
1244 De sousa oliveira S., Girard L., Raselli I., Anquetin J. In Press. Virtual reconstruction of a Late
1245 Jurassic metriorhynchid skull from Switzerland and its use for scientific illustration and paleoart.
1246 MorphoMuseuM
1247 Fitzinger, L. J. F. J. 1843. Systema Reptilium. Fasciculus Primus, Amblyglossae. Braumüller et
1248 Seidel, Vienna, 134 p.
1249 Foffa, D., Young, M.T., 2014. The cranial osteology of Tyrannoneustes lythrodectikos
1250 (Crocodylomorpha: Metriorhynchidae) from the Middle Jurassic of Europe. PeerJ 2, e608.
1251 Foffa, D., Young, M.T., Brusatte, S.L., Graham, M.R., Steel, L., 2018. A new metriorhynchid
1252 crocodylomorph from the Oxford Clay Formation (Middle Jurassic) of England, with
1253 implications for the origin and diversification of Geosaurini. Journal of Systematic
1254 Palaeontology 16, p. 1123–1143.
1255 Foffa, D., Young, M.T., Stubbs, T.L., Dexter, K.G., Brusatte, S.L., 2018b. The long-term
1256 ecology and evolution of marine reptiles in a Jurassic seaway. Nature Ecology & Evolution 2,
1257 1548–1555. https://doi.org/10.1038/s41559-018-0656-6
1258 Fraas, E., 1901. Die Meerkrokodile (Thalattosuchia n. g.) eine neue Sauriergruppe der
1259 Juraformation. Ahreshefte des Vereins für vaterländische Naturkunde in Württemberg 57, p. 409
1260 - 418
1261 Fraas, E., 1902. Die Meer-Crocodilier (Thalattosuchia) des oberen Jura unter specieller
1262 Berücksichtigung von Dacosaurus und Geosaurus. Palaeontographica 49, p. 1–71.
1263 Frey, B., Buchy M-C, Stinnesbeck W., Guadalupe López-Oliva J., 2002. Geosaurus vignaudi
1264 n.sp. (Crocodyliformes: Thalattosuchia), first evidence of metriorhynchid crocodilians in the
1265 Late Jurassic (Tithonian) of central-east Mexico (State of Puebla). Canadian Journal of Earth
1266 Sciences. 39(10): 1467-1483. https://doi.org/10.1139/e02-060
1267 Gandola, R., Buffetaut, E., Monaghan, N., Dyke, G., 2006. Salt glands in the fossil crocodile
1268 Metriorhynchus. Journal of Vertebrate Paleontology 26, p. 1009–1010.
1269 Geoffroy Saint-Hilaire, E. 1831. Recherches sur de grands sauriens trouvés à l'état fossile aux
1270 confins maritimes de la Basse-Normandie, attribués d'abord au Crocodile, puis déterminés sous
1271 les noms de Teleosaurus et Steneosaurus. Mémoires de l'Academie des sciences 12, p. 1138

George, I.D., Holliday, C.M., 2013. Trigeminal nerve morphology in Alligator mississippiensis and Its significance for Crocodyliform facial sensation and evolution. The Anatomical Record 296, p. 670–680.
Goloboff, P.A., Catalano, S.A., 2016. TNT version 1.5, including a full implementation of phylogenetic morphometrics. Cladistics 32, 221–238.
Goloboff, P.A., Farris, J.S., Nixon, K.C., 2008. TNT, a free program for phylogenetic analysis Cladistics 24, p. 774–786.
Gower, D. J. 1999. The cranial and mandibular osteology of a new rauisuchian archosaur from the Middle Triassic of southern Germany. Stuttgarter Beiträge zur Naturkunde Serie B (Geologie und Paläontologie) 280, p. 1-49
Grange, D.R., Benton, M.J., 1996. Kimmeridgian metriorhynchid crocodiles from England. Palaeontology. 39, p. 497-514
Grigg, Gordon, Kirshner, D., 2015. Biology and Evolution of Crocodylians. CSIRO Publishing. 672 p.
Hay, O. P., 1930. Second Bibliography and Catalogue of the Fossil Vertebrata of North America, Vol II. Carnegie Institution of Washington Publication No. 390, Carnegie Institution of Washington, Washington, DC, 1074 p.
Herrera Y., 2015. Metriorhynchidae (Crocodylomorpha: Thalattosuchia) from Upper Jurassic–Lower Cretaceous of Neuquén Basin (Argentina), with comments on the natural casts of the brain. In: M. Fernández, Y. Herrera (Eds.) Reptiles Extintos - Volumen en Homenaje a Zulma Gasparini. Publicación Electrónica de la Asociación Paleontológica Argentina 15(1), p. 159–171.
Herrera, Y., Fernández, M.S., Gasparini, Z., 2013. Postcranial skeleton of Cricosaurus araucanensis (Crocodyliformes: Thalattosuchia): morphology and palaeobiological insights 15.
Herrera, Y., Fernández, M.S., Lamas, S.G., Campos, L., Talevi, M., Gasparini, Z., 2015. Morphology of the sacral region and reproductive strategies of Metriorhynchidae: a counter-inductive approach. Earth and Environmental Science Transactions of The Royal Society of Edinburgh 106, 247–255. https://doi.org/10.1017/S1755691016000165
Herrera, Y., Aiglstorfer, M., Bronzati, M., 2021a. A new species of Cricosaurus (Thalattosuchia: Crocodylomorpha) from southern Germany: the first threedimensionally preserved Cricosaurus skull from the Solnhofen Archipelago. Journal of Systematic Palaeontology 19(2), p. 145-167
Herrera, Y., Fernández, M.S., Vennari, V.V., 2021b. Cricosaurus (Thalattosuchia, Metriorhynchidae) survival across the J/K boundary in the High Andes (Mendoza Province, Argentina). Cretaceous Research 118, 104673. https://doi.org/10.1016/j.cretres.2020.104673
Holliday, C.M., Witmer, L.M., 2007. Archosaur adductor chamber evolution: Integration of musculoskeletal and topological criteria in jaw muscle homology. Journal of Morphology 268, p. 457–484. https://doi.org/10.1002/jmor.10524
Johnson, Michela & Young, Mark & Steel, Lorna & Foffa, Davide & Smith, Adam & Hua, Stéphane & Havlik, Philipe & Howlett, Eliza & Dyke, Gareth. 2017. Re-description of 'Steneosaurus' obtusidens Andrews, 1909, an unusual macrophagous teleosaurid crocodylomorph

from the Middle Jurassic of England. Zoological Journal of the Linnean Society. 182. 1-34. 10.1093/zoolinnean/zlx035.
Krebs, B., 1967. Der Jura-KrokodilierMachimosaurus H. v. Meyer. Paläontol. Z. 41, 46–59. https://doi.org/10.1007/BF02998548
Lepage, Y., Buffetaut, E., Hua, S., Martin, J.E., Tabouelle, J., 2008. Catalogue descriptif, anatomique, géologique et historique des fossiles présentés à l'exposition « Les Crocodiliens fossiles de Normandie » (6 novembre - 14 décembre 2008). Bulletin de la Société Géologique de Normandie et des Amis du Muséum du Havre, tome 95, fascicule 2, p. 5-152.
Lydekker, R., 1889. On the remains and affinities of five genera of Mesozoic reptiles. Quarterly Journal of the Geological Society, 45, p. 41-59.
Maddison, W. P. and D.R. Maddison. 2019. Mesquite: a modular system for evolutionary analysis. Version 3.61 http://www.mesquiteproject.org
Madzia, D., Sachs, S., Young, M. T., Lukeneder, A., Skupien, P., 2021. Evidence of two lineages of metriorhynchid crocodylomorphs in the Lower Cretaceous of the Czech Republic. Acta Palaeontologica Polonica 66(2).
Martin, J.E., Vincent, P., Falconnet, J., 2015. The taxonomic content of Machimosaurus (Crocodylomorpha, Thalattosuchia). Comptes Rendus Palevol 14, p. 305– 310. Meyer, H. von, 1845. System der fossilen Saurier [Taxonomy of fossil saurians]. Neues Jahrbuch für Mineralogie, Geognosie, Geologie und PetrefaktenKunde. p. 278-285
Marty, D., Hug, W., Iberg, A., Cavin, L., Meyer, C., Lockley, M., 2003. Preliminary Report on the Courtedoux Dinosaur Tracksite from the Kimmeridgian of Switzerland. Ichnos 10, 209–219. https://doi.org/10.1080/10420940390256212
Massare, J.A., 1987. Tooth Morphology and Prey Preference of Mesozoic Marine Reptiles. Journal of Vertebrate Paleontology 7, 121–137.
Owen, R., 1883. On the Cranial and Vertebral characters of the Crocodilian Genus plesiosuchus. Quarterly Journal of the Geological Society 40, p. 153-159
Parrilla-Bel, J., M. T. Young, M. Moreno-Azanza, and J. I. Canudo. 2013. The first metriorhynchid crocodylomorph from the Middle Jurassic of Spain, with implications for evolution of the subclade Rhacheosaurini. PLoS ONE, 8:e54275. doi: 10.1371/journal.pone.0054275.
Parrilla-Bel, J., Canudo, J.I., 2015. Postcranial elements of "Maledictosuchus riclaensis" (Thalattosuchia) from the Middle Jurassic of Spain. Journal of Iberian Geology 41, 31–40. https://doi.org/10.5209/rev_JIGE.2015.v41.n1.48653
Pierce, S.E., Angielczyk, K.D. and Rayfield, E.J., 2009. Shape and mechanics in thalattosuchian (Crocodylomorpha) skulls: implications for feeding behaviour and niche partitioning. Journal of Anatomy, 215: 555-576. https://doi.org/10.1111/j.1469-7580.2009.01137.x
Pol, D., Gasparini, Z., 2009. Skull anatomy of Dakosaurus andiniensis (Thalattosuchia: Crocodylomorpha) and the phylogenetic position of Thalattosuchia. Journal of Systematic Palaeontology 7(2), p. 163–197.

Prasad, G.V.R., de Lapparent de Broin, F., 2002. Late Cretaceous crocodile remains from Naskal (India): comparisons and biogeographic affinities. Annales de Paléontologie 88, 19–71. https://doi.org/10.1016/S0753-3969(02)01036-4
Püntener C, Anquetin J, Billon-Bruyat J-P. 2020. New material of "Eurysternidae" (Thalassochelydia, Pan-Cryptodira) from the Kimmeridgian of the Swiss Jura Mountains. Palaeovertebrata 43:e2. DOI: 10.18563/pv.43.1.e2.
Quenstedt, F. A., 1856. Sonst und jetzt: populäre Vorträge über Geologie. Laupp
Rieppel, O., 1979. Ein Geosaurus-fragment (Reptilia, Thalattosuchia) aus dem oberen Malm von Evilard bei Biel.
Ronquist, F., Teslenko, M., van der Mark, P., Ayres, D.L., Darling, A., Höhna, S., Larget, B., Liu, L., Suchard, M.A., Huelsenbeck, J.P., 2012. MrBayes 3.2: Efficient Bayesian phylogenetic inference and model choice across a large model space. Systematic Biology 61, p. 539–542.
Sachs, S., Young, M., Abel, P., Mallison, H., 2019. A new species of the metriorhynchid crocodylomorph Cricosaurus from the Upper Jurassic of southern Germany. Acta Palaeontologica Polonica 64. https://doi.org/10.4202/app.00541.2018
Sachs, S., Young, M., Abel, P., Mallison, H., 2021. A new species of Cricosaurus (Thalattosuchia, Metriorhynchidae) based upon a remarkably well-preserved skeleton from the Upper Jurassic of Germany. Palaeontologia Electronica. https://doi.org/10.26879/928
Schaefer, K., 2012. Variabilité de la morphologie dentaire des crocodiliens marins (Thalattosuchia) du Kimméridgien d'Ajoie (Jura, Suisse). Mémoire de Master (non-publié), Université de Fribourg. 111 p.
Schaefer, K., Billon-Bruyat, J.-P., Hug, W.A., Friedli, V., Püntener, C., 2018. Vertébrés mésozoïques: crocodiliens. Catalogue du patrimoine paléontologique jurassien - A16. 188 p. .
Sebens, K.P., 1987. The Ecology of Indeterminate Growth in Animals 37.
Spindler, F., R. Lauer, H. Tischlinger, and M. Mäuser. 2021. The integument of pelagic crocodylomorphs (Thalattosuchia: Metriorhynchidae). Palaeontologia Electronica, 24:a25. doi: 10.26879/1099.
Vignaud, P., 1997. La morphologie dentaire des thalattosuchia (Crocodylia, Mesosuchia).
von Arthaber, G., 1906. Beiträge zur kenntnis der organisation und der anpassungsercheinungen des genus Metriorhynchus.
Wagner, J. A., 1858. Neue Beiträge zur Kenntniss der urweltlichen Fauna des lithographischen Schiefers: Saurier (Vol. 8).
Waskow, K., Grzegorczyk, D., Sander, P.M., 2018. The first record of Tyrannoneustes (Thalattosuchia: Metriorhynchidae): a complete skull from the Callovian (late Middle Jurassic) of Germany. PalZ 92, p. 457–480.
Wilberg, E.W., 2012, Phylogenetic and morphometric assessment of the evolution of the longirostrine crocodylomorphs, The University of Iowa.
Wilkinson, L.E., Young, M.T., Benton, M.J., 2008. A new metriorhynchid crocodilian (Mesoeucrocodylia Thalattosuchia) from the Kimmeridgian (Upper Jurassic) of Wiltshire, UK. Palaeontology 51, p. 1307– 1333.

1390 Young, M.T., 2014. Filling the ‘Corallian Gap’: re-description of a metriorhynchid
1391 crocodylomorph from the Oxfordian (Late Jurassic) of Headington, England. Historical Biology
1392 26, p. 80–90.
1393 Young, M.T., Andrade, M.B., 2009. What is Geosaurus? Redescription of Geosaurus giganteus
1394 (Thalattosuchia: Metriorhynchidae) from the Upper Jurassic of Bayern, Germany. Zoological
1395 Journal of the Linnean Society, 157, p. 551–585.
1396 Young, M.T., Brusatte, S.L., Ruta, M., Andrade, M.B., 2010. The evolution of
1397 Metriorhynchoidea (Mesoeucrocodylia, Thalattosuchia): an integrated approach using geometric
1398 morphometrics, analysis of disparity, and biomechanics. Zoological Journal of the Linnean
1399 Society, 158, p. 801–859.
1400 Young, M.T., Bell, M.A., Andrade, M.B., Brusatte, S.L., 2011. Body size estimation and
1401 evolution in metriorhynchid crocodylomorphs: implications for species diversification and niche
1402 partitioning. Zoological Journal of the Linnean Society 18.
1403 Young, M.T., Brusatte, S.L., Beatty, B.L., Andrade, M.B., Desojo, J.B., 2012a. Tooth-on-tooth
1404 interlocking occlusion suggests macrophagy in the Mesozoic marine crocodylomorph
1405 Dakosaurus. The Anatomical Record 295, p. 1147–1158.
1406 Young, M.T., Brusatte, S.L., Andrade, M.B., Desojo, J.B., Beatty, B.L., Steel, L., Schoch, R.R.,
1407 2012b. The cranial osteology and feeding ecology of the metriorhynchid crocodylomorph genera
1408 Dakosaurus and Plesiosuchus from the Late Jurassic of Europe. PLOS ONE 7, 42.
1409 Young, M.T., Andrade, M.B., Brusatte, S.L., Sakamoto, M., Liston, J., 2013a. The oldest known
1410 metriorhynchid super-predator: a new genus and species from the Middle Jurassic of England,
1411 with implications for serration and mandibular evolution in predacious clades. Journal of
1412 Systematic Palaeontology 11, p. 475–513.
1413 Young, M.T., Andrade, M.B., Etches, S., Beatty, B.L., 2013b. A new metriorhynchid
1414 crocodylomorph from the Lower Kimmeridge Clay Formation (Late Jurassic) of England, with
1415 implications for the evolution of dermatocranium ornamentation in Geosaurini. Zoological
1416 Journal of the Linnean Society. 169, p. 820–848.
1417 Young, M.T., Steel, L., Brusatte, S.L., Foffa, D., Lepage, Y., 2014. Tooth serration
1418 morphologies in the genus Machimosaurus (Crocodylomorpha, Thalattosuchia) from the Late
1419 Jurassic of Europe. Royal Society Open Science. 1, 140269.
1420 Young, M.T., Foffa, D., Steel, L., Etches, S., 2019. Macroevolutionary trends in the genus
1421 Torvoneustes (Crocodylomorpha: Metriorhynchidae) and discovery of a giant specimen from the
1422 Late Jurassic of Kimmeridge, UK. Zoological Journal of the Linnean Society 189(2), p. 483-493.
1423 Young, M.T., Brignon, A., Sachs, S., Hornung, J.J., Foffa, D., Kitson, J.J.N., Johnson, M.M.,
1424 Steel, L., 2020a. Cutting the Gordian knot: a historical and taxonomic revision of the Jurassic
1425 crocodylomorph Metriorhynchus. Zoological Journal of the Linnean Society 192(2), p. 510-553.
1426 Young, M.T., Sachs, S., Abel, P., Foffa, D., Herrera, Y., Kitson, J.J.N., 2020b. Convergent
1427 evolution and possible constraint in the posterodorsal retraction of the external nares in pelagic
1428 crocodylomorphs. Zoological Journal of the Linnean Society 189, p. 494- 520.

Figure 1

Geographical map of the Ajoie region, Canton of Jura, Switzerland.

The excavation site of MJSN BSY008-465 (BSY, Courtedoux–Bois de Sylleux) is indicated along the A16 Transjurane highway (in gray).

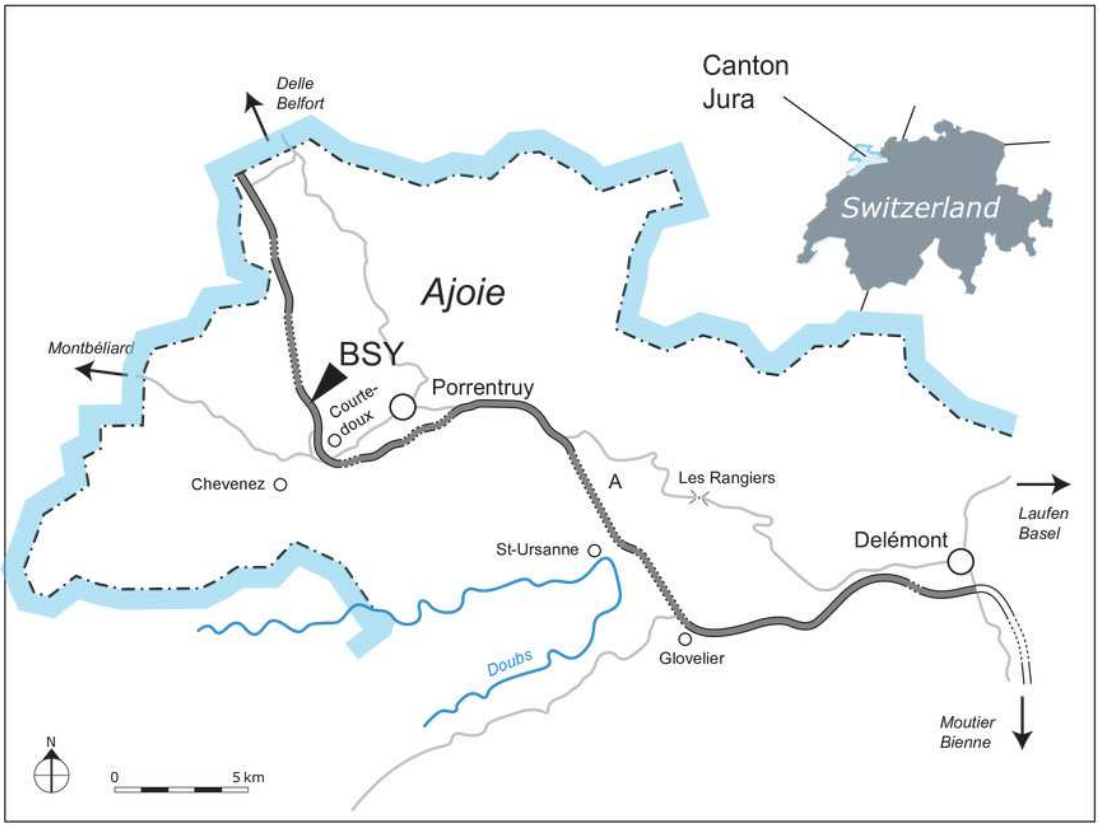

Figure 2

Taphonomical disposition of the metriorhynchid skeleton MJSN BSY008-465.

(a) photograph of the skeleton still embedded in the limestone block (see text); (b) drawing of the bones in their taphonomical position.

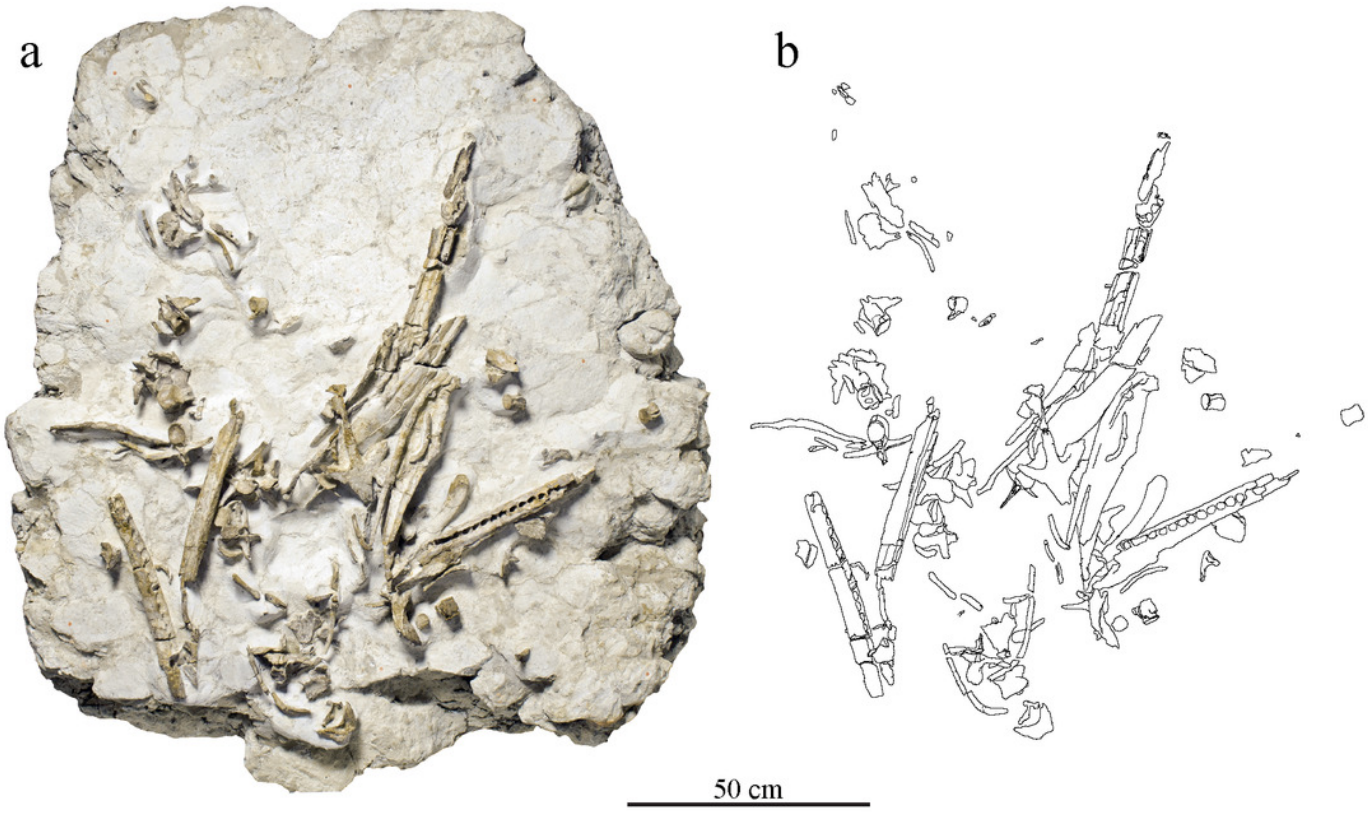

Figure 3

Stratigraphical section of the Reuchenette Formation in Ajoie, Canton of Jura, Switzerland, with a close-up on the Lower Virgula Marls.

MJSN BSY008-465 was found on the hardground level 4000 in the Lower Virgula Marls. The stratigraphical chart is derived from Comment et al. (2015) and Püntener et al. (2020).

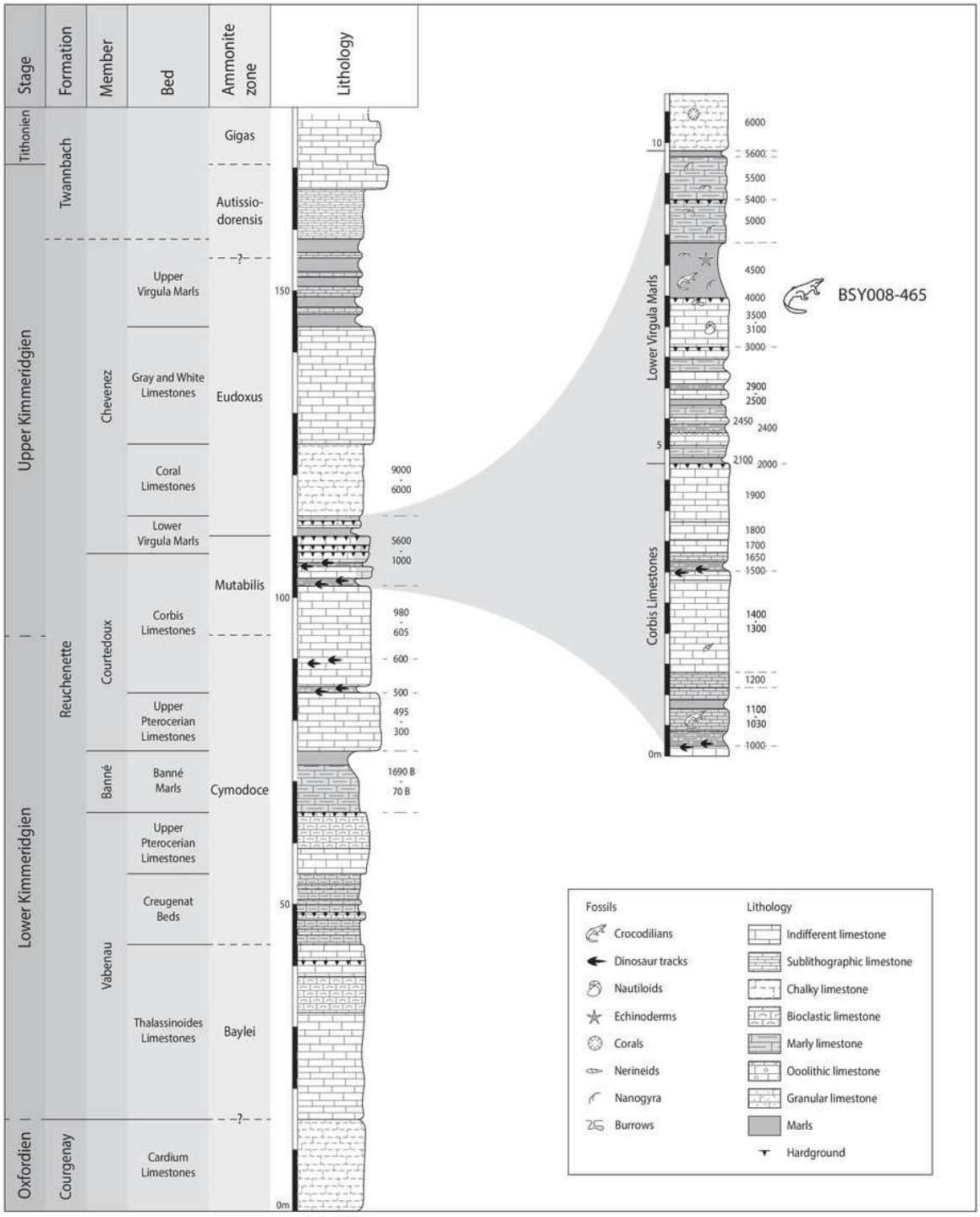
Stage
Formation
Member
Bed
Ammonite zone
Lithology
Tithonien
Upper Kimmeridgien
Lower Kimmeridgien
Oxfordien
Twannbach
Reuchenette
Courgenay
Chevenez
Courtedoux
Banné
Vabenau
Upper Virgula Marls
Gray and White Limestones
Coral Limestones
Lower Virgula Marls
Corbis Limestones
Upper Pterocerian Limestones
Banné Marls
Upper Pterocerian Limestones
Creugenat Beds
Thalassinoides Limestones
Cardium Limestones
Gigas
Autissiodorensis
Eudoxus
Mutabilis
Cymodoce
Baylei
9000
6000
5600
1000
980
605
600
500
495
300
1690 B
70 B
150
100
50
0m
Lower Virgula Marls
Corbis Limestones
BSY008-465
Fossils
Crocodilians
Dinosaur tracks
Nautiloids
Echinoderms
Corals
Nerineids
Nanogyra
Burrows
Lithology
Indifferent limestone
Sublithographic limestone
Chalky limestone
Bioclastic limestone
Marly limestone
Ooolithic limestone
Granular limestone
Marls
Hardground

Figure 4

MJSN BSY008-465, holotype of *Torvoneustes jurensis* (Kimmeridgian, Porrentruy, Switzerland).

Scientific drawings of the reconstructed skull (a) and mandible (b) in dorsal and (c) lateral views. Remaining matrix is represented in yellow. Anterior to the right. Abbreviations: **al**, alveolus; **an**, angular; **art**, articular; **cp**, coronoid process; **den,** dentary; **fr**, frontal; **mx**, maxillary; **na**, nasal; **pa**, parietal; **pmx**, premaxillary; **po**, postorbital; **prf**, prefrontal; **san**: surangular; **sdg**: surangulodentary groove **sq**, squamosal; **spl**, splenial; **tc**, tooth crown.

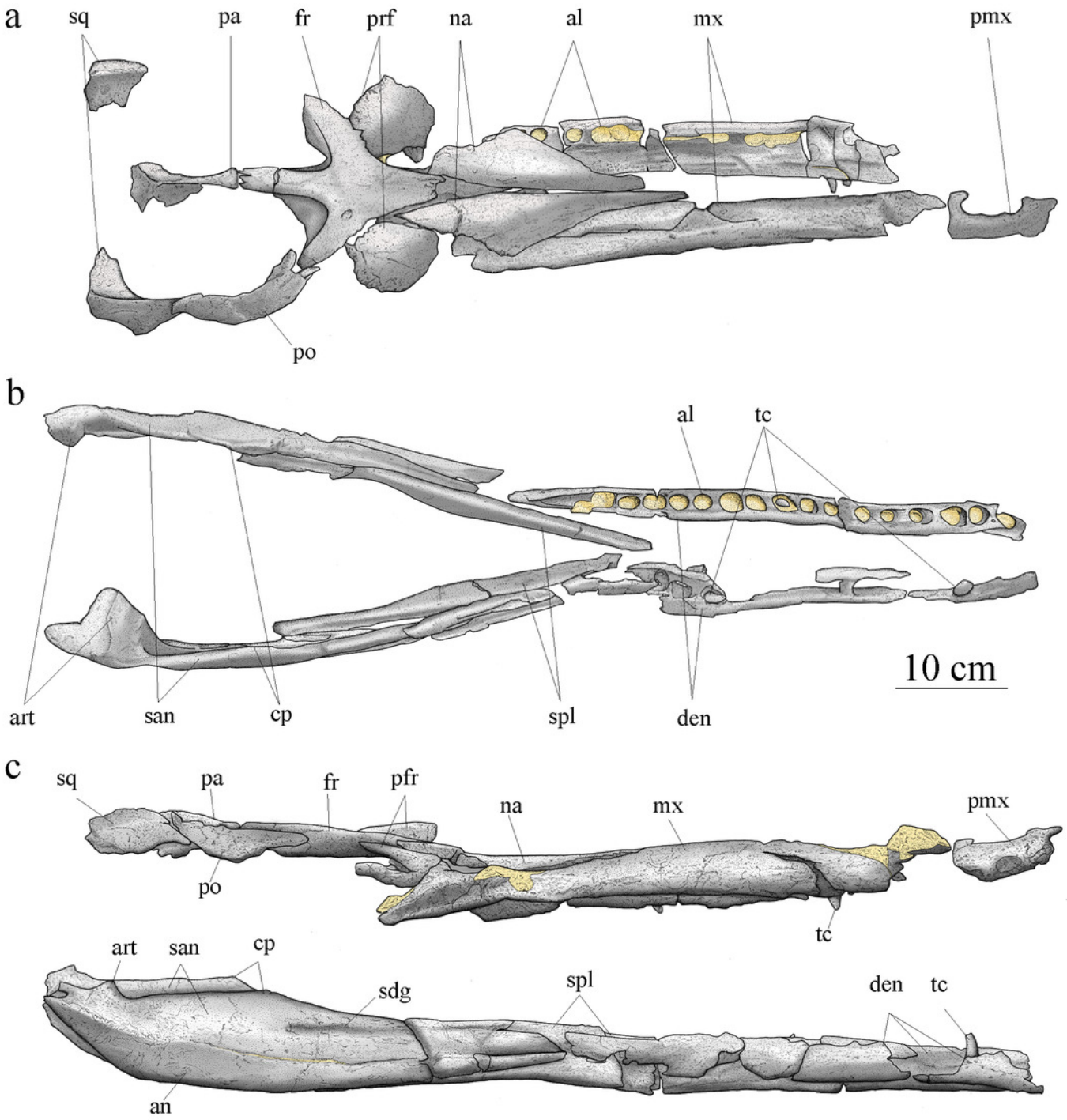
a
sq
pa
fr
prf
na
al
mx
pmx
po
b
al
tc
art
san
cp
spl
den
10 cm
c
sq
pa
fr
pfr
na
mx
pmx
po
tc
art
san
cp
sdg
spl
den
tc
an

Figure 5

MJSN BSY008-465, holotype of *Torvoneustes jurensis* (Kimmeridgian, Porrentruy, Switzerland).

(a) Left nasal, (b) right nasal, (c) right prefrontal, and (d) right premaxilla in dorsal views. Anterior to the right.

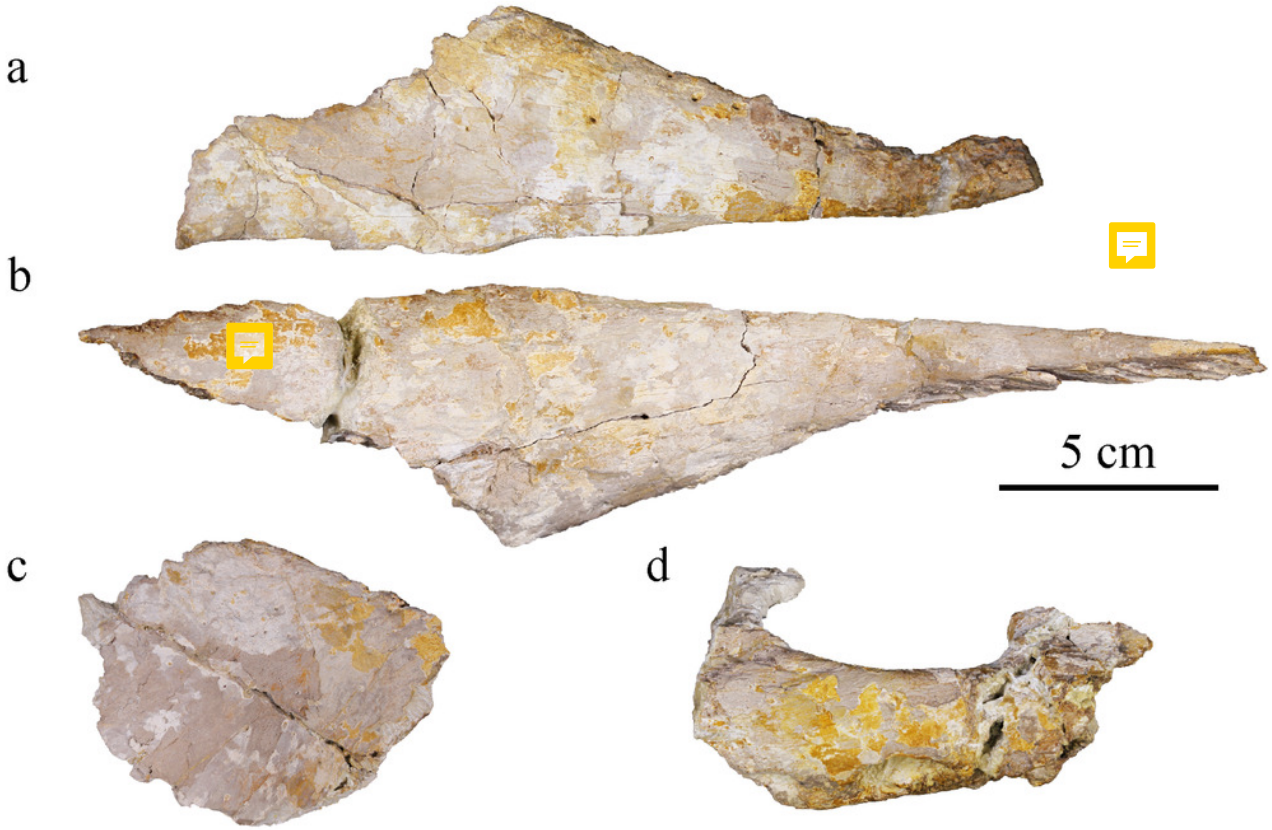

Figure 6

MJSN BSY008-465, holotype of *Torvoneustes jurensis* (Kimmeridgian, Porrentruy, Switzerland).

Scientific drawings and photographs of the right maxilla in (a, b) ventral and (c, d) lateral views. Anterior to the right. Abbreviations: **al**, alveolus; **for**, foramen; **mx**, maxilla; **no**, notch; **pa**, palatine. Numbers indicate the preserved alveoli. Matrix is in yellow.

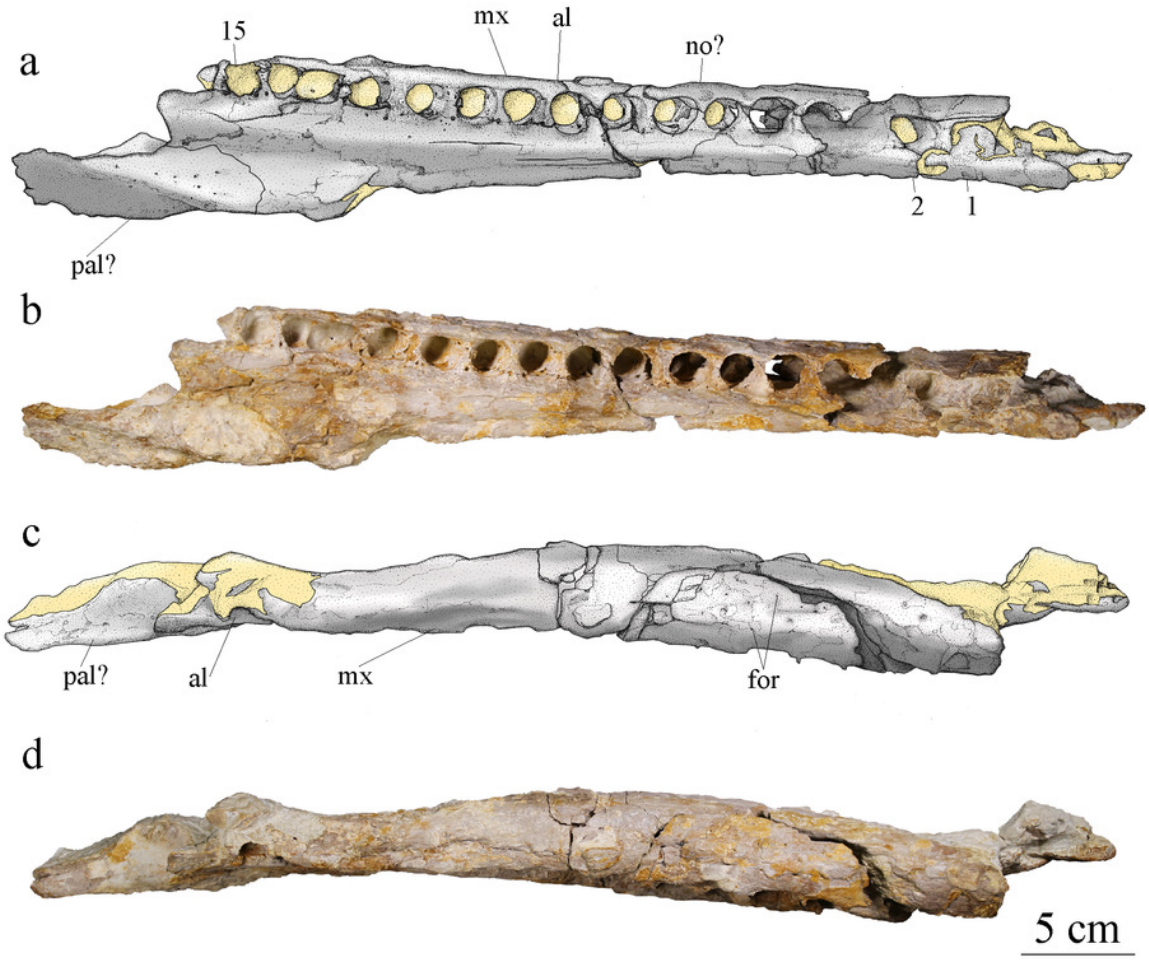

Figure 7

MJSN BSY008-465, holotype of *Torvoneustes jurensis* (Kimmeridgian, Porrentruy, Switzerland).

(a) Scientific drawing, (b) interpretative drawing and (c) photograph of the frontal and left prefrontal in dorsal view. The angle formed by the lateral contacts of the frontal with the prefrontal and nasal is indicated in (b). Abbreviation: **fr**, frontal; **if**, intertemporal flange; **prf**, prefrontal. Matrix is in yellow.

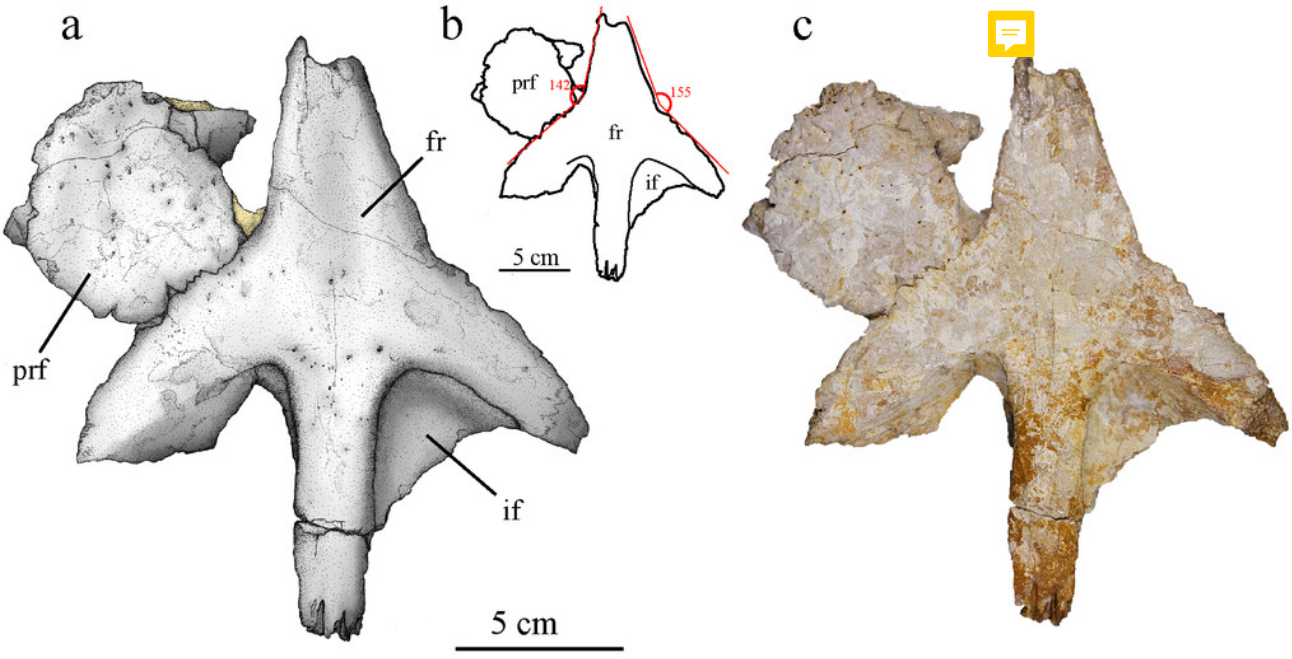

Figure 8

MJSN BSY008-465, holotype of *Torvoneustes jurensis* (Kimmeridgian, Porrentruy, Switzerland).

Posterior cranial elements with the right postorbital in (a) dorsal, (b) medial, and (c) lateral views; the parietal in (d) right lateral and (e) dorsal view; and the right squamosal in (f) dorsal view. Anterior to the right (except in b to the left). Abbreviations: **in**, incision; **sqfs**, squamosal flat surface.

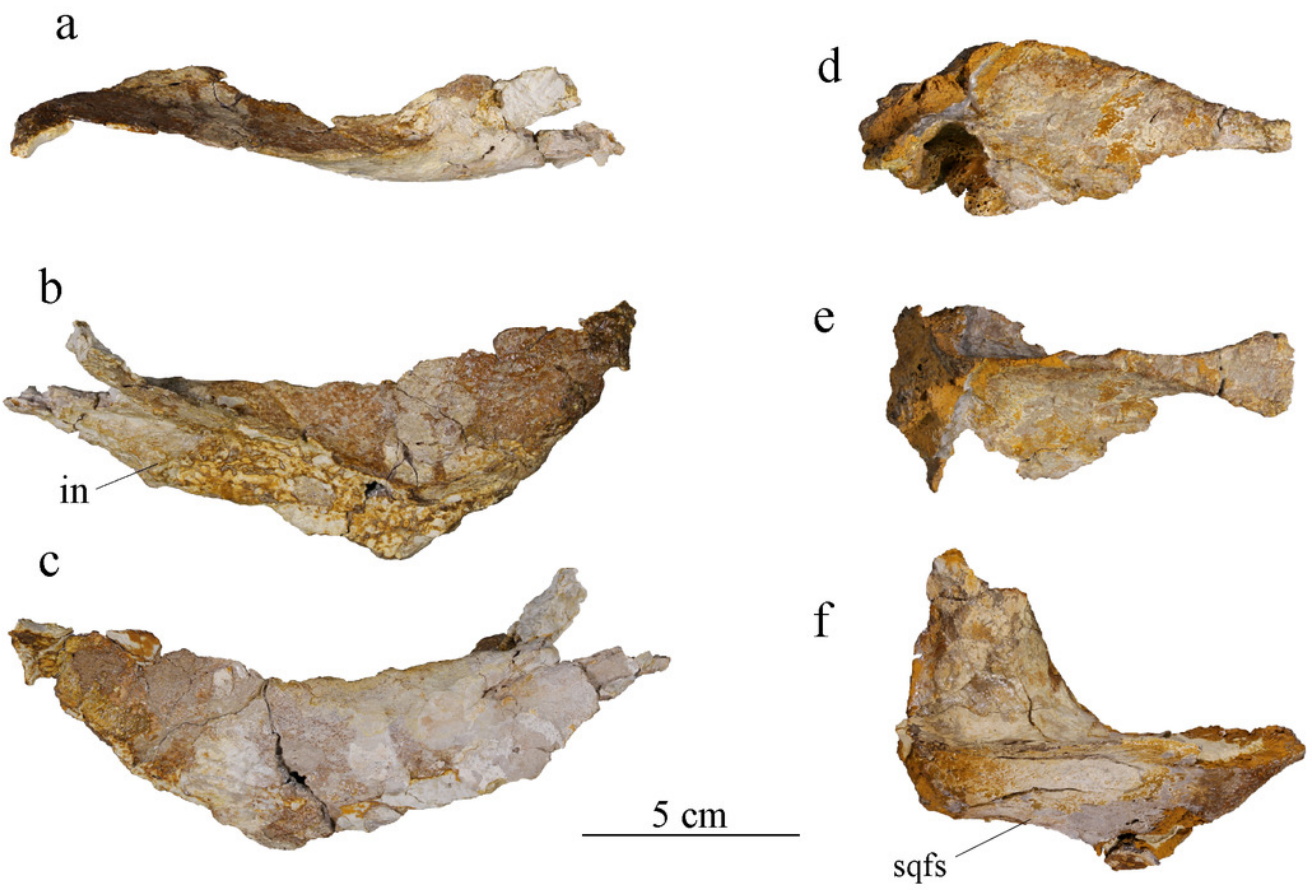

Figure 9

MJSN BSY008-465, holotype of *Torvoneustes jurensis* (Kimmeridgian, Porrentruy, Switzerland).

Photographs of the right splenial in (a) lateral, (b) medial, and (c) dorsal views. Photograph of the left splenial in (d) medial view. Abbreviations: **for**, foramen; **sym**, symphysis.

Figure 10

MJSN BSY008-465, holotype of *Torvoneustes jurensis* (Kimmeridgian, Porrentruy, Switzerland).

Scientific drawings of the left dentary in (a) dorsal and (b) lateral views. Photographs of the left dentary in (c) dorsal and (d) lateral views. Anterior to the left. Abbreviations: **al**, alveolus; **for**, foramen; **sdg**, surangulodentary groove; **tc**, tooth crown. Matrix is in yellow.

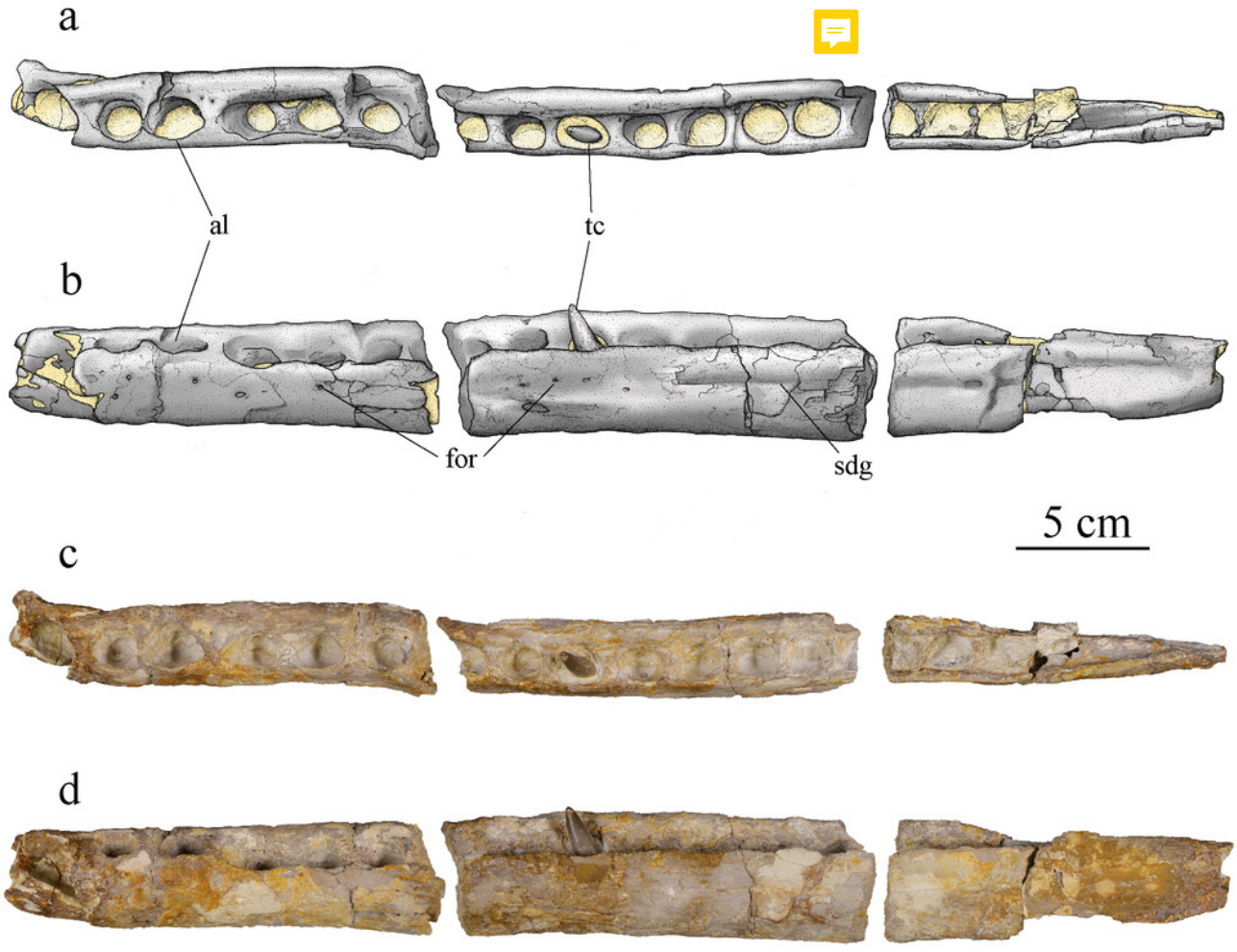

Figure 11

MJSN BSY008-465, holotype of *Torvoneustes jurensis* (Kimmeridgian, Porrentruy, Switzerland).

Scientific drawings of the posterior part of the right ramus of the mandible in (a) medial, (b) dorsal, and (c) lateral views. Photographs of the posterior part of the right ramus of the mandible in (d) medial, (e) dorsal, and (f) lateral views. Abbreviations: **an**, angular; **art**, articular; **cp**, coronoid process; **for**, foramen; **gf**, glenoid fossa; **pra**, prearticular; **ret**, retroarticular process; **san**, surangular; **sdg**, surangulodentary groove. Matrix is in yellow.

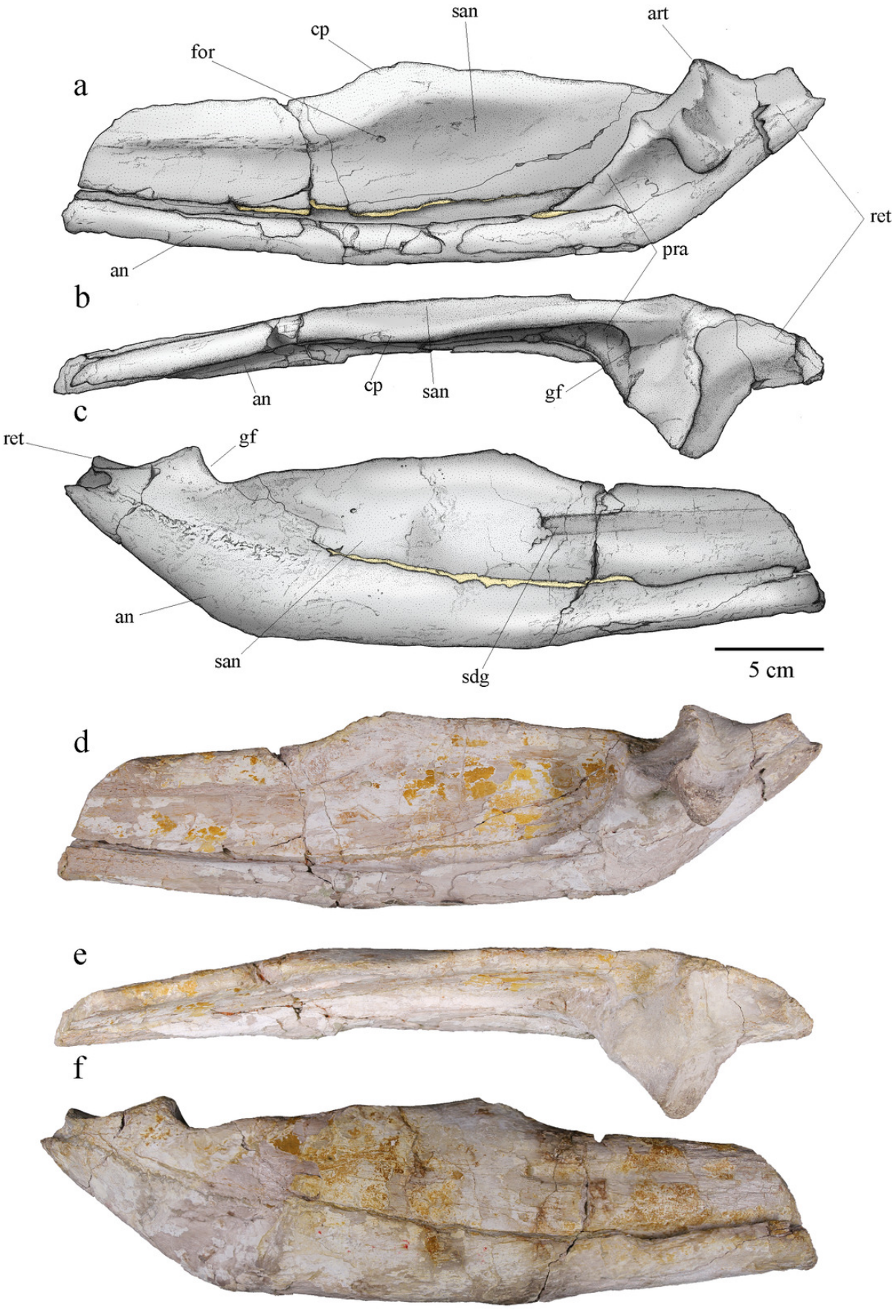
a
b
c
d
e
f
san
art
cp
for
ret
pra
an
cp
san
gf
an
ret
gf
san
sdg
5 cm

Figure 12

MJSN BSY008-465, holotype of *Torvoneustes jurensis* (Kimmeridgian, Porrentruy, Switzerland).

Two of the best-preserved isolated teeth in (a) lateral and (b) probably anterior views.

Abbreviations: **c**, crown; **ca**, carina; **r**, root.

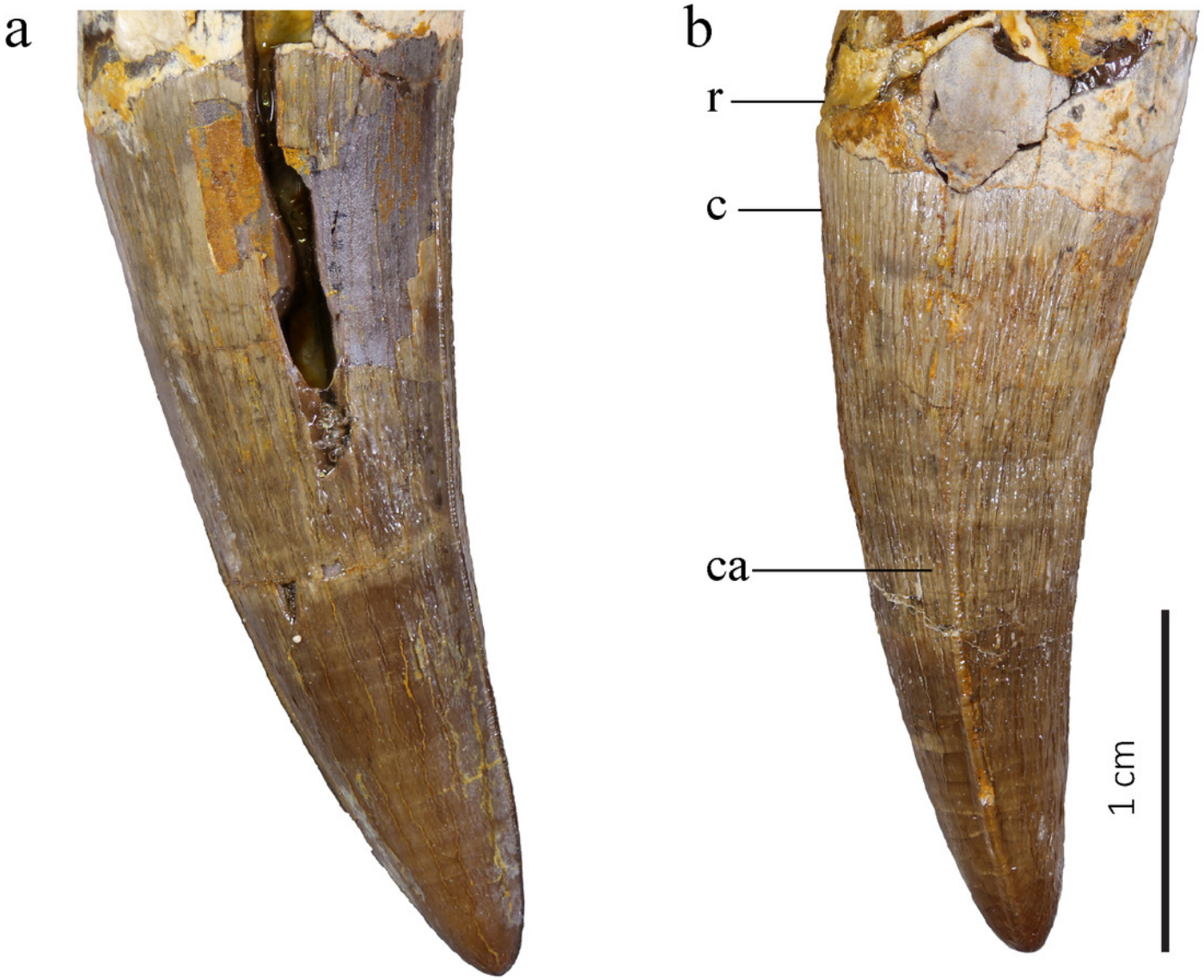

Figure 13

MJSN BSY008-465, holotype of *Torvoneustes jurensis* (Kimmeridgian, Porrentruy, Switzerland).

Microscopic photographs of MJSN BSY008-465 teeth. (a, b) mid-upper tooth crown; (c) tooth apex; (d) tooth base.

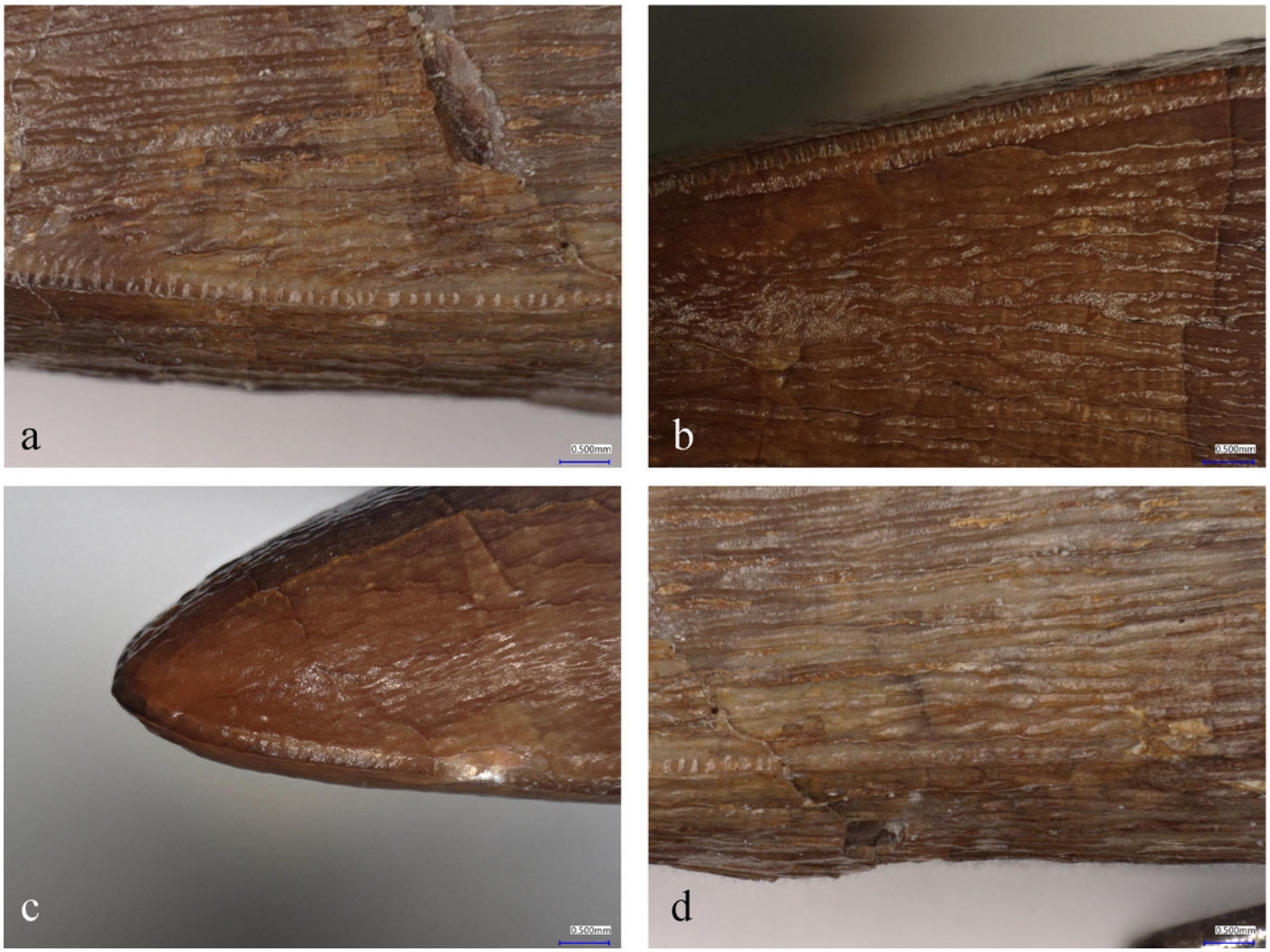

Figure 14

MJSN BSY008-465, holotype of *Torvoneustes jurensis* (Kimmeridgian, Porrentruy, Switzerland).

Cervical vertebra in (a) anterior and (b) right lateral views; dorsal vertebra in (c) anterior and (d) right lateral views; anterior caudal vertebra in (e) anterior and (f) right lateral views; Posterior caudal vertebrae in (g) anterior and (h) right lateral views. Abbreviations: **di**, diapophysis; **pa**, parapophysis; **prz**, prezygapophysis; **pz**, postzygapophysis.

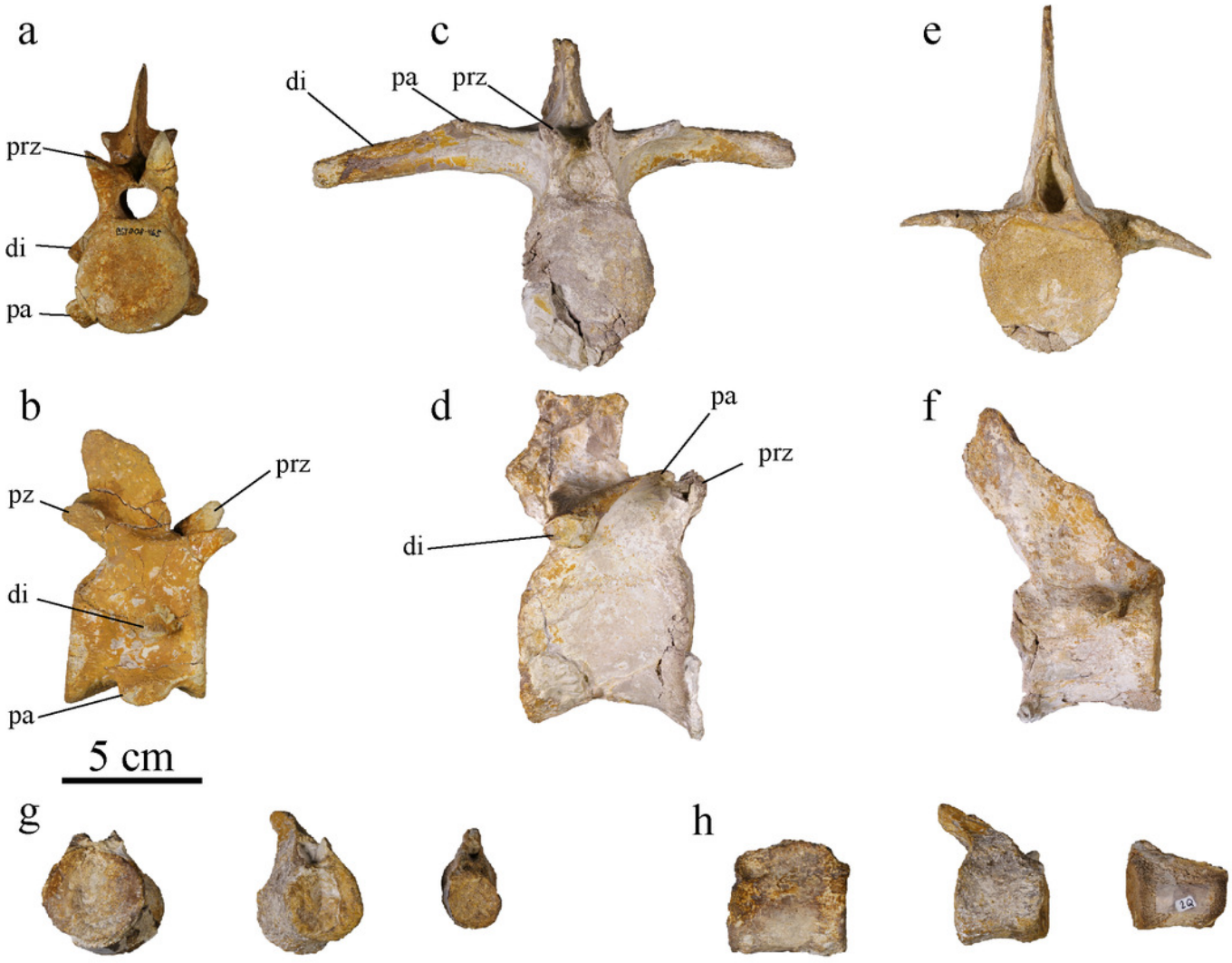

Figure 15

MJSN BSY008-465, holotype of *Torvoneustes jurensis* (Kimmeridgian, Porrentruy, Switzerland).

(a, b) dorsal ribs, (c–e) cervical ribs; chevron in (f) dorsal and (g) lateral views (anterior to the top).

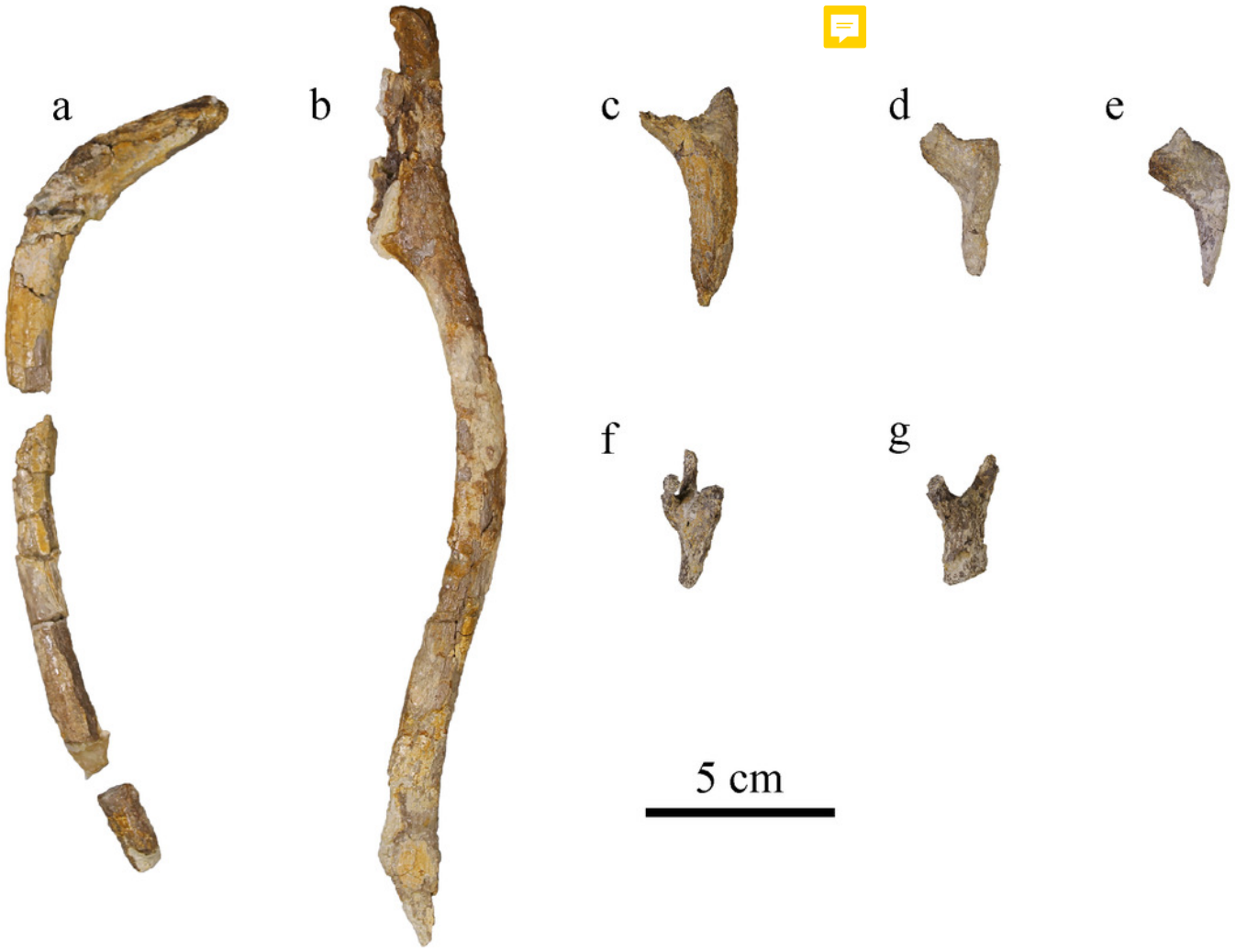

Figure 16

MJSN BSY008-465, holotype of *Torvoneustes jurensis* (Kimmeridgian, Porrentruy, Switzerland).

Right femur in (a) medial and (b) lateral views; (c) left ischium in lateral view; (d) right fibula in lateral view.

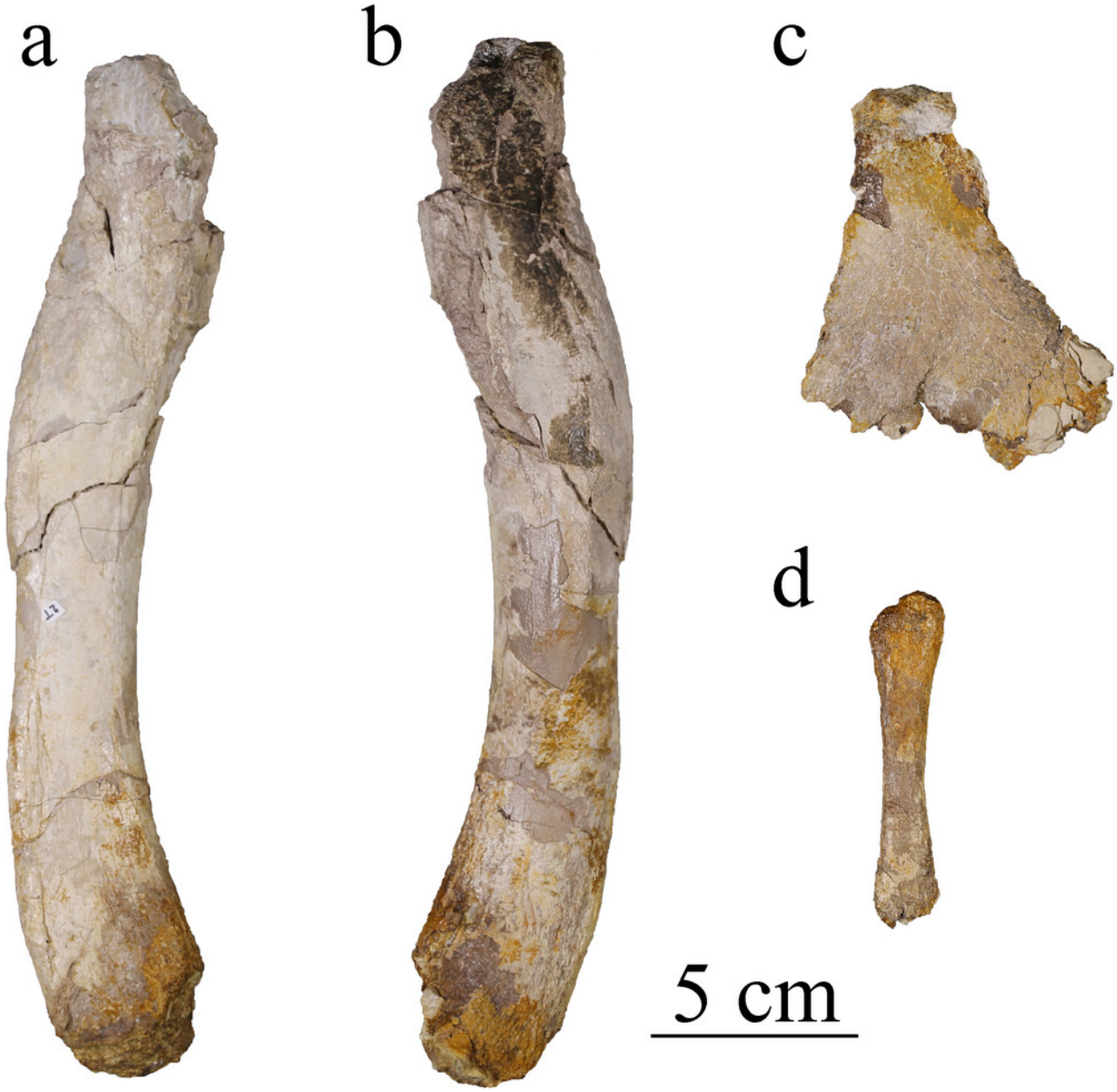
a
b
c
d
5 cm

Figure 17

Phylogenetic placement of MJSN BSY008-465 (*Torvoneustes jurensis* sp. nov.) within Geosaurinae in the parsimony analyses.

(a) strict consensus topology for the unweighted analysis; (b) strict consensus topology for the strongly downweighted analyses (k = 1 and k = 3), (c) strict consensus topology for the moderately downweighted analyses (k = 7 and k = 10); (d) strict consensus topology for the moderately to weakly downweighted analyses (k = 15, k = 20 and k = 50). Numbers indicate clades: 1. Geosaurinae, 2. Geosaurini, 3. E-clade. Complete strict consensus trees are provided in supplementary material S1.

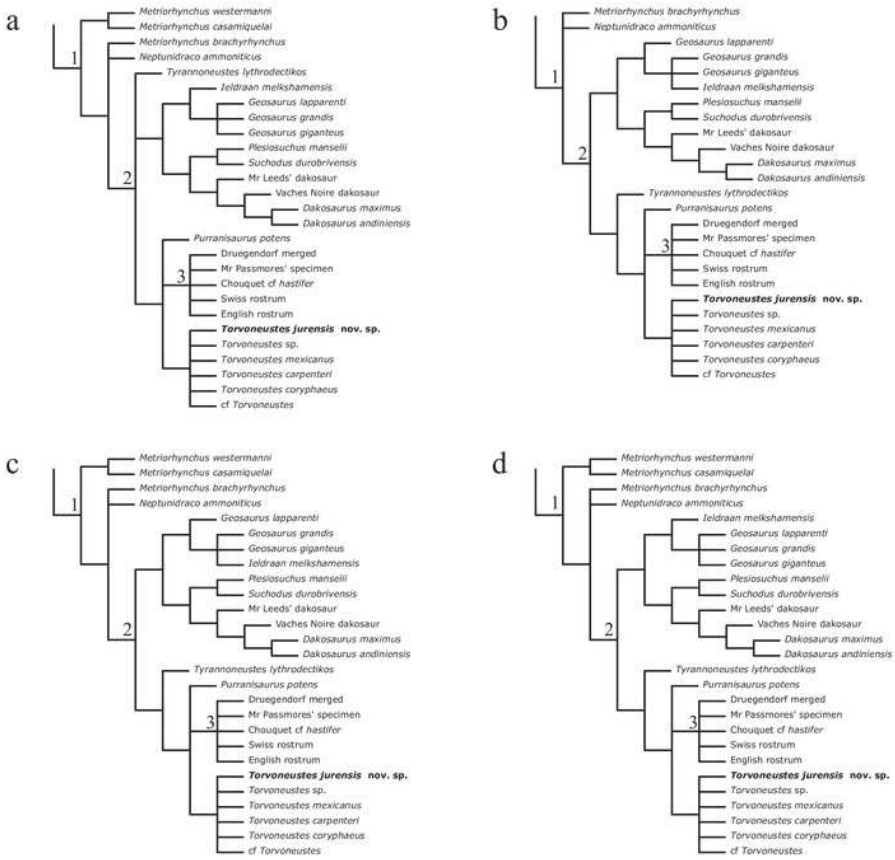
a
Metriorhynchus westermanni
Metriorhynchus casamiquelai
Metriorhynchus brachyrhynchus
Neptunidraco ammoniticus
Tyrannoneustes lythrodectikos
Ieldraan melkshamensis
Geosaurus lapparenti
Geosaurus grandis
Geosaurus giganteus
Plesiosuchus manselii
Suchodus durobrivensis
Mr Leeds' dakosaur
Vaches Noire dakosaur
Dakosaurus maximus
Dakosaurus andiniensis
Purranisaurus potens
Druegendorf merged
Mr Passmores' specimen
Chouquet cf hastifer
Swiss rostrum
English rostrum
Torvoneustes jurensis nov. sp.
Torvoneustes sp.
Torvoneustes mexicanus
Torvoneustes carpenteri
Torvoneustes coryphaeus
cf Torvoneustes
1
2
3
b
Metriorhynchus brachyrhynchus
Neptunidraco ammoniticus
Geosaurus lapparenti
Geosaurus grandis
Geosaurus giganteus
Ieldraan melkshamensis
Plesiosuchus manselii
Suchodus durobrivensis
Mr Leeds' dakosaur
Vaches Noire dakosaur
Dakosaurus maximus
Dakosaurus andiniensis
Tyrannoneustes lythrodectikos
Purranisaurus potens
Druegendorf merged
Mr Passmores' specimen
Chouquet cf hastifer
Swiss rostrum
English rostrum
Torvoneustes jurensis nov. sp.
Torvoneustes sp.
Torvoneustes mexicanus
Torvoneustes carpenteri
Torvoneustes coryphaeus
cf Torvoneustes
1
2
3
c
Metriorhynchus westermanni
Metriorhynchus casamiquelai
Metriorhynchus brachyrhynchus
Neptunidraco ammoniticus
Geosaurus lapparenti
Geosaurus grandis
Geosaurus giganteus
Ieldraan melkshamensis
Plesiosuchus manselii
Suchodus durobrivensis
Mr Leeds' dakosaur
Vaches Noire dakosaur
Dakosaurus maximus
Dakosaurus andiniensis
Tyrannoneustes lythrodectikos
Purranisaurus potens
Druegendorf merged
Mr Passmores' specimen
Chouquet cf hastifer
Swiss rostrum
English rostrum
Torvoneustes jurensis nov. sp.
Torvoneustes sp.
Torvoneustes mexicanus
Torvoneustes carpenteri
Torvoneustes coryphaeus
cf Torvoneustes
1
2
3
d
Metriorhynchus westermanni
Metriorhynchus casamiquelai
Metriorhynchus brachyrhynchus
Neptunidraco ammoniticus
Ieldraan melkshamensis
Geosaurus lapparenti
Geosaurus grandis
Geosaurus giganteus
Plesiosuchus manselii
Suchodus durobrivensis
Mr Leeds' dakosaur
Vaches Noire dakosaur
Dakosaurus maximus
Dakosaurus andiniensis
Tyrannoneustes lythrodectikos
Purranisaurus potens
Druegendorf merged
Mr Passmores' specimen
Chouquet cf hastifer
Swiss rostrum
English rostrum
Torvoneustes jurensis nov. sp.
Torvoneustes sp.
Torvoneustes mexicanus
Torvoneustes carpenteri
Torvoneustes coryphaeus
cf Torvoneustes
1
2
3

Figure 18

Phylogenetic placement of MJSN BSY008-465 (*Torvoneustes jurensis* sp. nov.) within Geosaurinae after pruning of unstable taxa.

(a) maximum agreement subtree for the unweighted analysis; (b) maximum agreement subtree for the strongly downweighted analyses (k = 1 and k = 3); (c) maximum agreement subtree for the moderately downweighted analyses (k = 7 and k = 10); (d) maximum agreement subtree for the moderately to weakly downweighted analyses (k = 15, k = 20 and k = 50). Numbers indicate clades: 1. Geosaurinae, 2. Geosaurini, 3. E- clade <!--[if !supportAnnotations]--> [AJ1] <!--[endif]-->. Complete pruned consensus trees are provided in supplementary material <!--[if !supportAnnotations]--> <!--[endif]--> <!--[if !supportAnnotations]--> <!--[endif]--><!--[if !supportAnnotations]--> <!--[endif]--> <!--[if !supportAnnotations]--> [AJ1] <!--[endif]-->Les arbres complets sont-ils donnés en annexe ? Si oui, ajouter le même genre de phrase que pour la fig 17 en adaptant <!--[if !supportAnnotations]--> <!--[endif]-->

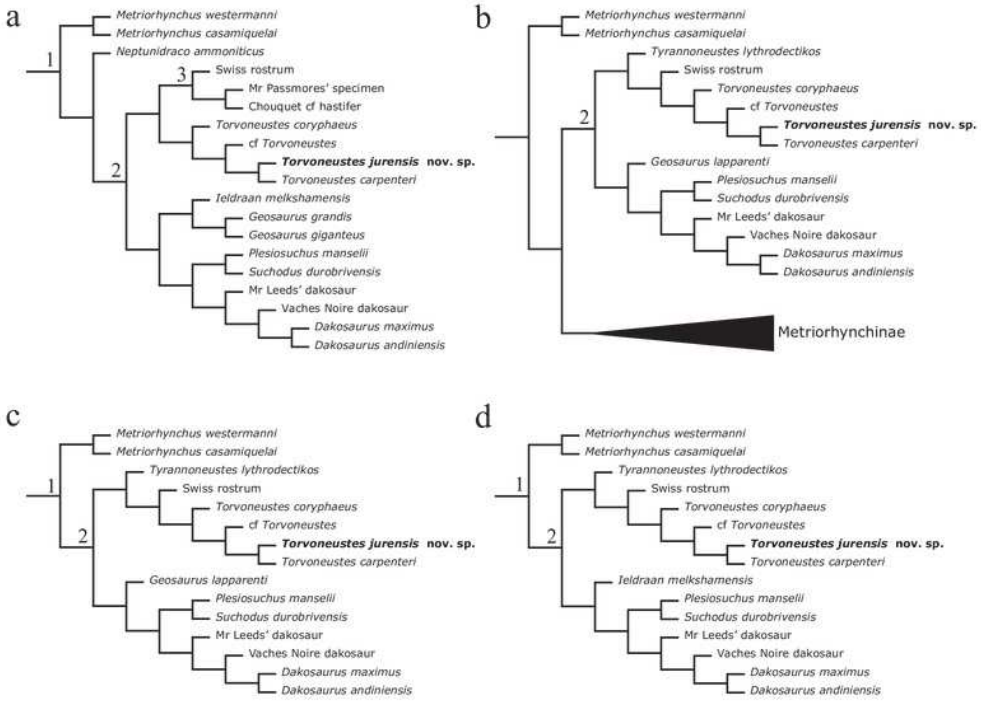
a
Metriorhynchus westermanni
Metriorhynchus casamiquelai
Neptunidraco ammoniticus
Swiss rostrum
Mr Passmores' specimen
Chouquet cf hastifer
Torvoneustes coryphaeus
cf Torvoneustes
Torvoneustes jurensis nov. sp.
Torvoneustes carpenteri
Ieldraan melkshamensis
Geosaurus grandis
Geosaurus giganteus
Plesiosuchus manselii
Suchodus durobrivensis
Mr Leeds' dakosaur
Vaches Noire dakosaur
Dakosaurus maximus
Dakosaurus andiniensis
1
2
3
b
Metriorhynchus westermanni
Metriorhynchus casamiquelai
Tyrannoneustes lythrodectikos
Swiss rostrum
Torvoneustes coryphaeus
cf Torvoneustes
Torvoneustes jurensis nov. sp.
Torvoneustes carpenteri
Geosaurus lapparenti
Plesiosuchus manselii
Suchodus durobrivensis
Mr Leeds' dakosaur
Vaches Noire dakosaur
Dakosaurus maximus
Dakosaurus andiniensis
Metriorhynchinae
2
c
Metriorhynchus westermanni
Metriorhynchus casamiquelai
Tyrannoneustes lythrodectikos
Swiss rostrum
Torvoneustes coryphaeus
cf Torvoneustes
Torvoneustes jurensis nov. sp.
Torvoneustes carpenteri
Geosaurus lapparenti
Plesiosuchus manselii
Suchodus durobrivensis
Mr Leeds' dakosaur
Vaches Noire dakosaur
Dakosaurus maximus
Dakosaurus andiniensis
1
2
d
Metriorhynchus westermanni
Metriorhynchus casamiquelai
Tyrannoneustes lythrodectikos
Swiss rostrum
Torvoneustes coryphaeus
cf Torvoneustes
Torvoneustes jurensis nov. sp.
Torvoneustes carpenteri
Ieldraan melkshamensis
Plesiosuchus manselii
Suchodus durobrivensis
Mr Leeds' dakosaur
Vaches Noire dakosaur
Dakosaurus maximus
Dakosaurus andiniensis
1
2

Figure 19

Phylogenetic placement of MJSN BSY008-465 (*Torvoneustes jurensis* sp. nov) within Metriorhynchidae in the Bayesian analysis

Numbers in red represent node support values. Numbers on the tree branches indicate clades: 1. Metriorhynchidae, 2. Geosaurinae and 3. Geosaurini. Complete tree is provided in supplementary material.

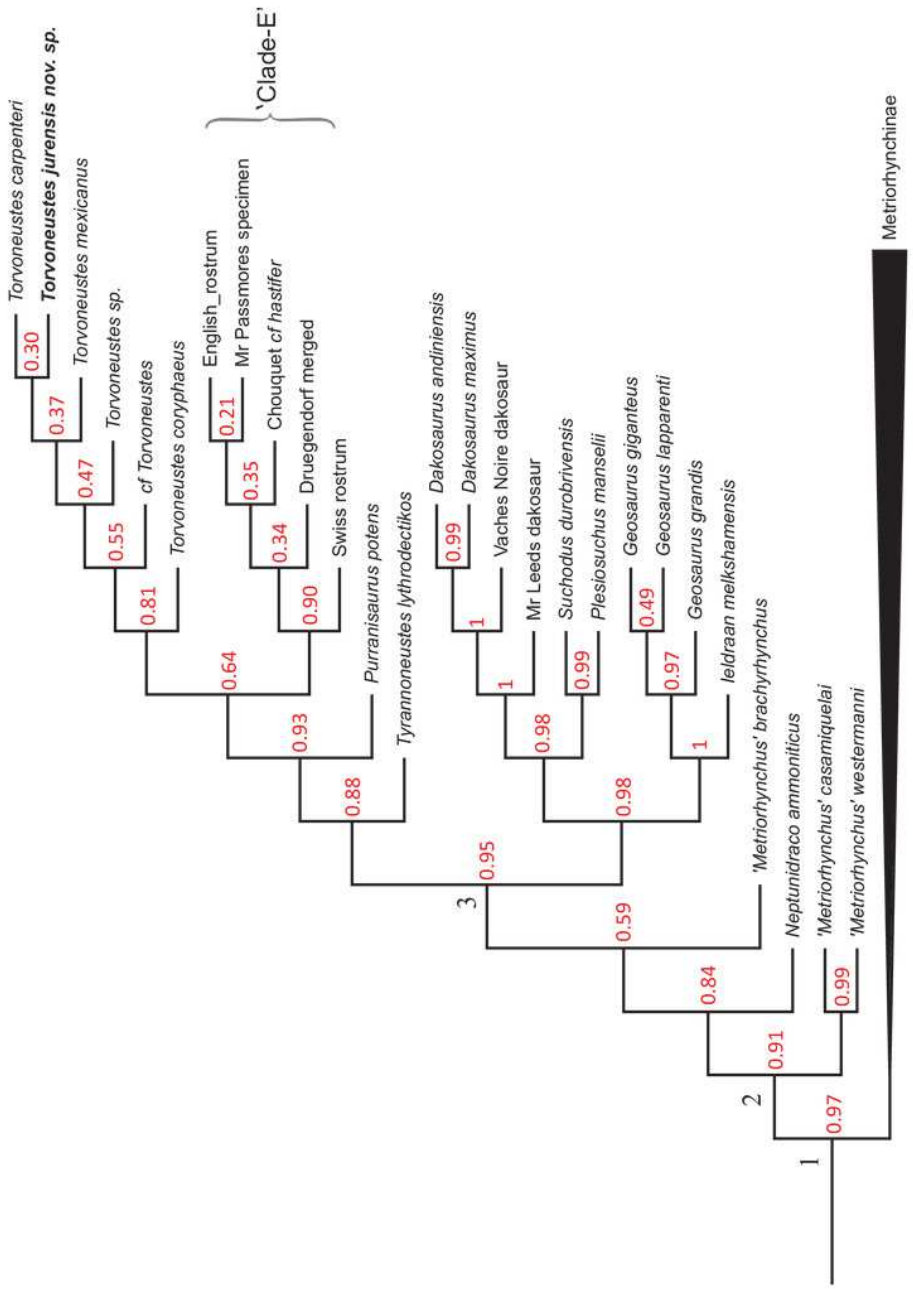
Torvoneustes carpenteri
Torvoneustes jurensis nov. sp.
Torvoneustes mexicanus
Torvoneustes sp.
cf Torvoneustes
Torvoneustes coryphaeus
English_rostrum
Mr Passmores specimen
Chouquet cf hastifer
Druegendorf merged
Swiss rostrum
Purranisaurus potens
Tyrannoneustes lythrodectikos
Dakosaurus andiniensis
Dakosaurus maximus
Vaches Noire dakosaur
Mr Leeds dakosaur
Suchodus durobrivensis
Plesiosuchus manselii
Geosaurus giganteus
Geosaurus lapparenti
Geosaurus grandis
Ieldraan melkshamensis
'Metriorhynchus' brachyrhynchus
Neptunidraco ammoniticus
'Metriorhynchus' casamiquelai
'Metriorhynchus' westermanni
Metriorhynchinae
'Clade-E'
0.30
0.37
0.47
0.55
0.81
0.64
0.21
0.35
0.34
0.90
0.93
0.88
0.99
1
1
0.98
0.99
0.98
0.49
0.97
1
0.59
3
0.95
0.84
0.91
2
0.99
0.97
1

Figure 20

Life reconstruction of Torvoneustes jurensis MJSN BSY008-465 in its paleoenvironment.

Artwork by SDSO.

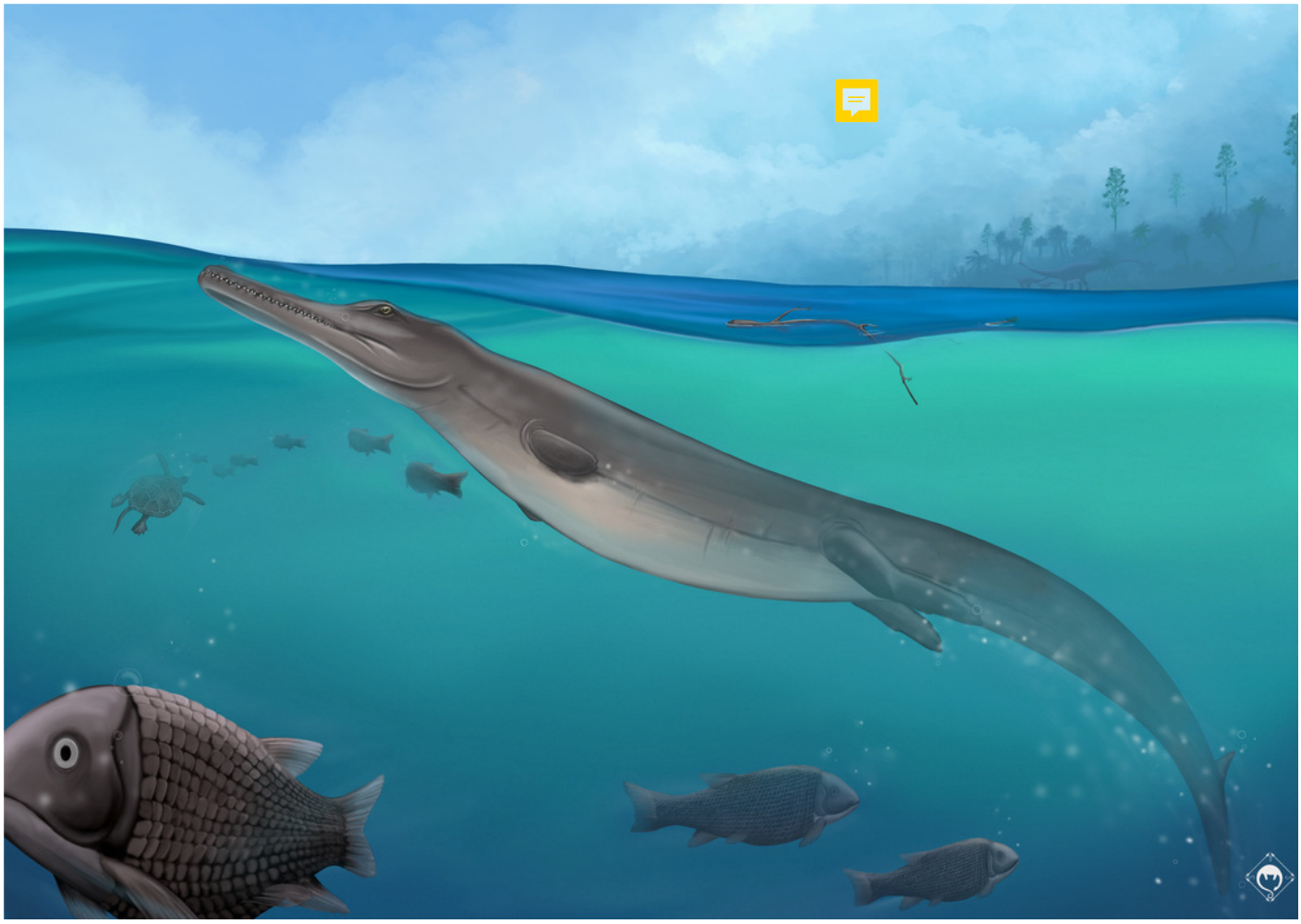

Table 1 (on next page)

Overview of the Kimmeridgian-Lower Tithonian metriorhynchids species and a few of their dental characteristics.

Gracilineustes acutus is excluded from the table due to the lack of information. The specimen was lost during WW2, the same goes for *Rhacheosaurus gracilis* NHMUK PV R 3948 for whom the teeth or alveaoli are indistinguishable, while R*hacheosaurus cf gracilis* LF 2426 skull is not entierly represented. Therein the distinction between "true ziphodont" and "false ziphodont" condition as defined by Andrade *et al.*, 2010 is not specified. The estimated tooth count is from the referred articles; the denticle density for *Dakosaurus maximus* and *Geosaurus grandis* from *Andrade et al., 2010* and for *Torvoneustes mexicanus* from Barrientos-Lara et al., 2016.

Family	Metriorhynchinae									Geosaurinae								
Tribe	Rhacheosaurinae									Geosaurini								
Species	*Cricosaurus suevicus* (Fraas, 1901, 1902, SMNS 9808)	*Cricoaurus albersdoerferi* (Sachs *et al.*, 2021, BMMS-BK 1-2)	*Cricosaurus elegans* (Wagner, 1852, BSPG AS I 504)	*Cricosaurus bambergensis* (Sachs *et al.*, 2019, NKMB-P-Watt 14/274)	*Cricosaurus rauhuti* (Herrera *et al.*, 2021, SNSB-BSPG 1973 I 195)	*Maledictosuchus nuyiviiana* (Barrientos-Lara *et al.*, 2018, IGM 4863)	*Cricosaurus' saltillensis* (Buchy *et al.*, 2013, MUDECPC 487)	*Metriorhynchus palpebrosus* (Phillips, 1871, Grange & Benton, 1996, (OUMNH J.29823)	Metriorhynchus Geoffroyii (Me. Brevirostris) (Young *et al.*, 2020; MHNG V-2232)	*Metriorhynchus'* cf *hastifer* (Chouquet cf *'hastifer'*, Lepage *et al.*, 2008, Eudes-Deslongchamps, 1867)	*Dakosaurus maximus* (Young *et al.*, 2012, SMNS 8203)	*Plesiosuchus manselii* (Young *et al.*, 2012, NHMUK PV OR 40103)	*Geosaurus giganteus* (Young & Andrade, 2009, NHMR.12299, NHM3700	*Geosaurus grandis* (Young et al., 2012, BSPG AS-VI-1)	*Torvoneustes carpenteri* (Grange & Benton, 1996, BRSMG Ce17365)	*Torvoneustes coryphaeus* (Young *et al.*, 2013, MJML K1863)	*Torvoneustes mexicanus* (Barrientos-Lara *et al.*, 2016, IGM 9026)	MJSNBSY0 08-465

													20)					
Age	Upper Kimmeridgian	Upper Kimmeridgian	Lower Tithonian	Upper Kimmeridgian	Lower Tithonian	Kimmeridgian	Lower Tithonian	Lower Tithonian	Lower Kimmeridgian	Kimmeridgian	Upper Kimmeridgian	Upper Kimmeridgian	Lower Tithonian	Lower Tithonian	Upper Kimmeridgian	Lower Kimmeridgian	Kimmeridgian	Upper Kimmeridgian
Country	Germany	Germany	Germany	Germany	Germany	Mexico	Mexico	United Kingdom	France	France	Germany	United Kingdom	Germany	Germany	United Kingdom	United Kingdom	Mexico	Switzerland
Tethor namentation	Smooth	Smooth	Smooth	Smooth	Wellspaced, lowlongitudinalridges	Smooth labial side. discontinuous low apicobasal ridges on	faintapicobasallyalignedsubparallelridges	?	?	Conspicious apicobasal ridges	Overall smooth	Low relief apicobasal ridges	Overall smooth	Smooth	Conspicious apicobasal ridges	Conspicious apicobasal ridges	Conspicious apicobasal ridges	Conspicious apicobasal ridges

						the lingual surface												
Carinae	Yes, faint	Yes, faint	Yes, faint	Yes, faint	Yes, at least unicarenate	Yes	Yes, faint	?	?	Yes	Yes, prominent	Yes, prominent	Yes, prominent	Yes, prominent	Yes, prominent	Yes, prominent	Yes, prominent	Yes, prominent
Denticules	No	No	No	No	No	No	No	?	?	?	Yes	Yes	Yes	Yes	Yes	Yes	Yes	Yes
Zipho donti e	/	/		/	/	/	/	?	?	?	Macro	Micro	Micro	Micro	Micro	Micro	Micro	Micro
Denticules density (number of denticle/5 mm)	/	/		/	/	/	/	?	?		16-18	?	?	28, 1	?	?	30	30-40

Maxillary tooth count (absolute)	26	23		23	/	17	12	25 (OUMNHJ.29823)-27	14	20?	13	14	12 (NHM37020)	14	11	11	5	15
Maxillary tooth count (estimated)		23+		23+	/	26?	17	/	20+? (half of the rostrum is easily missing)	20+?		14 to 18	12+		14	17-19		Up to 21
Dentary tooth count (absolute)	24	22		18+	/	/	15	14	/	/	12	13	7 (NHM37020)		/	/	4	16
Dentary tooth co		22+		18+	/	/	~15?	14+	/	/			7+		/	/		Up to 17

unt (estimated)																		
Taphonomic condition	Complete specimen in limestone	Complete specimen in limestone	Skull in limestone	Complete specimen in limestone	Incomplete skull	Incomplete skull	Disarticulated skull	Skull. No teeth remaining	Anterior half of the rostrum, no teeth remaining	complete skull	Incomplete skull	Incomplete skull	NHMR.1229: middle portion of the skull and mandible, deformed. NHM		Heavily crushed, incomplete skull	Incomplete skull, hlaf of the rostrum missing	Fragmentary rostrum	Disarticulated skull

													37020: skull and mandible in limestone.					

1

Table 2 (on next page)

Descriptives statistics of the cladograms resulting from the parsimony analysis.

In the unwieghted analysis, the number of Most Parsimonious Cladograms is higher than the storage capicity (20 000).

K	Number of MPCs	Length	CI	RI	RC	HI
-		2417	0,334	0,803	0,268	0,666
1	297	2072	0,389	0,845	0,329	0,611
3	297	2065	0,391	0,846	0,331	0,609
7	99	2044	0,395	0,848	0,335	0,605
10	99	2044	0,395	0,848	0,335	0,605
15	33	2034	0,397	0,85	0,337	0,603
20	33	2033	0,397	0,85	0,337	0,603
50	33	2033	0,397	0,85	0,337	0,603

1